FEBEX

Ciemat

UAM
UNIVERSIDAD AUTONOMA
DE MADRID

CIEMAT/DIAE/54111/4/99 v1

Report 70-IMA-M-0-5 v1

THERMO-HYDRO-GEOCHEMICAL TESTS ON SMALL CELLS

AUTHORS:
Jaime Cuevas
María Victoria Villar
Marta Martín
Juan Carlos Cobeña
Santiago Leguey
Pedro Rivas

November 2000

FEBEX

Ciemat

UAM
UNIVERSIDAD AUTONOMA
DE MADRID

CIEMAT/DIAE/54111/4/99 v1

Report 70-IMA-M-0-5 v1

THERMO-HYDRO-GEOCHEMICAL TESTS ON SMALL CELLS

PREPARADO (Prepared)	REVISADO (Revised)	APROBADO (Approved)
FECHA (Date): November 2000	**FECHA (Date): November 2000**	**FECHA (Date): November 2000**
FIRMA (Signature): J. Cuevas, M. V. Villar, M. Martín, J. C. Cobeña	**FIRMA (Signature):** S. Leguey, P. Rivas	**FIRMA (Signature):** P. Rivas

THERMO-HYDRO-GEOCHEMICAL TESTS ON SMALL CELLS

Index

Figures

Tables

1. ABSTRACT

In the context of an investigation of the near field for a repository of high-level radioactive waste, the FEBEX Project, a set of laboratory tests has been designed to give a better understanding of the thermo-hydro-mechanical and geochemical behaviour of the compacted bentonite. Small compacted samples of bentonite are heated during variable periods of time, of up to 80 days, under different thermal gradients. The hydration water is either granitic, simulating the conditions of the outer part of the barrier, or saline, which simulates the chemistry of the pore waters inside the bentonite barrier. At the end of the thermo-hydraulic (TH) treatment, a geochemical characterisation is performed in different sections, both of the soluble components and of the solid phase. The microstructure is analysed by means of optical microscopy and determination of the BET surface and pore size distribution. The swelling capacity of the whole sample and its permeability are also checked. The results of the permeability and swelling tests are compared to those obtained in experiments performed under the same conditions with non-treated samples.

As a result of hydration, there exists a rapid movement of chloride towards the heater. This ion is progressively excluded of the bentonite after saturation, what makes the bulk salinity of the clay decrease. Anion exclusion should prevent the anion transport once the bentonite is saturated, but the existence of preferential passages is postulated to explain the continuous salinity decrease. This phenomenon makes the salt content in the compacted bentonite very limited, with localised anomalies prior to saturation. All the physico-chemical parameters that have been determined are virtually unchanged during the TH treatment.

An increase of the hydraulic conductivity after the TH treatment with saline water has been observed, while the swelling capacity of the samples treated with granitic water slightly increases after treatment.

2. INTRODUCTION

The aim of FEBEX (Full-scale Engineered Barriers Experiment) is to study the behaviour of components in the near-field for a high-level radioactive waste (HLW) repository in crystalline rock. The experimental work consists of three main parts:

- an “in situ” test, under natural conditions and at full scale;
- a “mock-up” test, at almost full scale; and
- a series of laboratory tests to complement the information from the two large-scale tests.

The project is based on the Spanish disposal reference concept for disposal of radioactive waste in crystalline rock (AGP Granito): the waste canisters are placed horizontally in drifts and surrounded by a clay barrier constructed from highly-compacted bentonite blocks (ENRESA 1995).

The engineered barriers (waste, canister, and clay barrier) are key elements in the final disposal concept for HLW. The matrix of the spent fuel acts as a reducing barrier that minimises solubility; the canister isolates the wastes for a certain time and contributes to the reducing environment. The clay barrier has the multiple purpose of providing mechanical stability for the canister, by absorbing stress and deformations, of sealing discontinuities in the adjacent rock and retarding the arrival of groundwater at the canister and of retaining/retarding the migration of the radionuclides released, once failure of the canister and lixiviation of the spent fuel have occurred.

The behaviour of a HLW repository is determined, to a large extent, by the characteristics of the design and construction of the engineered barriers and especially by the changes that may occur in the mechanical, hydraulic, and geochemical properties as a result of the combined effects of heat generated by the radioactive decay and of the water and solutes contributed by the surrounding rock. Therefore, it has been considered of fundamental importance that the processes taking place in the near-field be understood and quantified, for the evaluation of long-term behaviour.

In previous R&D plans, ENRESA has studied the sources of supply of materials to be used in the clay barrier, as well as their thermal, hydraulic, mechanical, and geochemical behaviour. Integral characterisation studies of granite masses have also been carried out. As a result of these studies, and given the fact that to date there has not been any large-scale experiment in granite with the waste canisters placed horizontally in drifts, ENRESA has reached the conclusion that the next step, in establishing the viability of the concept and in progressing in the comprehension and evaluation of the behaviour of the near-field (especially of the clay barrier), is the performance of a very complete experiment, such as FEBEX.

Therefore, the FEBEX experiment has the multiple objectives of demonstrating the feasibility of fabricating and assembling the engineered barriers and of developing methodologies and models for evaluation of the thermo-hydro-mechanical (THM) and thermo-hydro-geochemical (THG) behaviour of the near-field. These objectives are to be attained through the combination of the “in situ”, “mock-up”, and laboratory tests. These tests constitute the main parts of the experiment, according to the program designed by ENRESA.

Fundamentally, the objective of the demonstration is expected to be attained in the “in situ” test, which operates under natural conditions with components constructed with the actual design dimensions of a repository drift. The demonstration objective has less importance in the “mock-up” test.

The objectives of checking the predictive capacities of the THM and THG numerical models will be supported by the program of laboratory tests designed to study and comprehend the processes that take place in the clay barrier under simple and controlled conditions and to develop the governing equations. The “mock-up” test, performed at almost full scale and with well-known geometry, along with well-controlled initial and boundary conditions, will serve to verify the predictive capacity of the coupled numerical models and serve also as a reference for the evaluation of discrepancies, if they exist, and for adjustment of the models predicting the behaviour of the clay barrier under more heterogeneous conditions, such as those in the existing natural system of the “in situ” test.

The underground laboratory managed by NAGRA (Grimsel, Switzerland) has been selected for performance of the “in situ” test, due to the similarity of the Spanish and Swiss reference concepts for the repository and the suitable laboratory conditions for this test. The “mock-up” test is being performed at the CIEMAT facilities (Madrid, Spain). The laboratory tests are being performed at various research facilities (UPC-DIT, CSIC-Zaidín, CIEMAT, and GRS).

Among these tests are included those performed in cells in which the compacted bentonite is subjected simultaneously to heating and hydration, in opposite directions, for different periods of time. The object of these tests is to analyse the properties of the bentonite and its behaviour under conditions that will be found in a repository. The precipitation of mineral phases due to local changes in the chemical equilibrium and the hydration itself can produce changes in the salinity of the interstitial water and in the microstructural organisation of the clay particles. The hydraulic and mechanical properties of the bentonite can be modified by the special conditions of the barrier.

In the Buffer Mass Test performed at Stripa, several possible chemical changes were envisaged: charge change through replacement of Si by Al in the montorillonite thetrahedrons, migration and precipitation of the released silica, and formation of mixed layer (I/S) by K-fixation (Pusch 1985). The determination of the hydraulic conductivity and of the swelling pressure was considered a valuable check of the preservation of the original properties of the bentonite, even if they are not very sensitive methods. After 1 year of heating the saturated clay at 125 °C, no change in physical properties was observed, although slight indication of silica precipitation was reported.

Melamed et al. (1992) found that compacted sodium bentonite hydrated and heated at a temperature of 75 °C during several months, suffered a migration of sodium out of the bentonite, replaced by other cations by cation exchange reactions. Dissolution/precipitation of sulphur compounds and dissolution of gypsum and carbonates were also observed.

In a series of tests, similar to those presented here, in which the compacted bentonite was submitted to simultaneous heating and hydration (Villar et al. 1996, Cuevas et al. 1997) a redistribution of salts was observed, in which advection as water comes in, convection near the heater and diffusion by concentration gradients were invoked as the main mechanisms. The exchange complex was also modified by the thermal gradient.

This report is a summary of the main results and conclusions found during the FEBEX Project in the tests performed in small thermo-hydraulic cells. More detailed data can be found in the following FEBEX reports:

- CUEVAS, J & VILLAR, M.V.(1997): Diseño y fabricación del equipo experimental para ensayos termo-hidro-geoquímicos en celdas pequeñas. *Informe Técnico CIEMAT-IMA 54A15/5/97*. 70-IMA-L-0-38. 10 pp.

- CUEVAS, J.; VILLAR, M.V. & HIDALGO, D.(1997): Metodología de los ensayos termo-hidro-geoquímicos en celdas pequeñas. *Informe Técnico CIEMAT-DIAE* 54A10/4/97. 70-IMA-L-0-47.

- CUEVAS, J. & MARTÍN, M.(1998): Ensayos THG en celdas. Resultados de los ensayos en celdas pequeñas de transporte con agua granítica. CIEMAT/DIAE/54111/8/98. FEBEX report 70-IMA-L-0-54.

- CUEVAS, J. & MARTÍN, M.(1999): Ensayos THG en celdas. Resultados de los ensayos de transporte con agua salina. CIEMAT/DIAE/54111/6/99. FEBEX report 70-IMA-L-0-63.

- CUEVAS, J.; COBEÑA, J.C. & MARTÍN, M.(1999): Ensayos THG en celdas. Resultados de los ensayos de fábrica con agua granítica y salina. CIEMAT/DIAE/54111/7/99. FEBEX report 70-IMA-L-0-64.

- VILLAR, M.V.(1999): Ensayos THG en celdas. Resultados de los ensayos de permeabilidad e hinchamiento con agua granítica. CIEMAT/DIAE/54111/8/99. FEBEX report 70-IMA-L-0-55.

- VILLAR, M.V.(1999): Ensayos THG en celdas. Resultados de los ensayos de permeabilidad e hinchamiento con agua salina. CIEMAT/DIAE/54111/5/99. FEBEX report 70-IMA-L-0-65.

3. MATERIAL

The tests have been performed in a bentonite coming from the Cortijo de Archidona deposit (Almería, Spain) which has been selected by ENRESA as suitable material for the backfilling and sealing of HLW repositories. It is the same than the clay used for the FEBEX Project in the in-situ (Grimsel, Switzerland) and the mock-up (Madrid, Spain) tests (ENRESA 1998), i.e., the clay of reference 70-IMA-3-4-0. The processing at the factory has consisted in disaggregation and gently grinding, drying at 60 °C and sieving by 5 mm.

3.1. MINERALOGY

The FEBEX bentonite has a content of montmorillonite higher than 90 %. Besides, it contains variable quantities of quartz, plagioclase, K-feldspar, calcite and opal-CT (cristobalite-trydimite). The bulk mineralogy, as well as a more detailed quantification of the accesory minerals, have been performed by means of XRD and polarising optical microscopy (automatic and semiautomatic image analysis). The techniques of quantification can be followed in Schultz (1964), Barahona (1974) and Drees and Ransom (1994). Table I shows the results of the XRD quantification for several size fractions in the bentonites. The data obtained by both UAM and CIEMAT laboratories are compared.

Table I: Mineralogical composition (F2: <2 μm size fraction; F50: >50 μm fraction; UAM, CIEMAT: bulk sample 70-IMA-3-4-0; (*) smectite, mica and chlorite)

FEBEX	smectite	cristobalite	quartz	plagioclase	K-feldspar	calcite	trydimite
F2	> 99	-	-		-	-	
F50	28 (*)	-	16	16	40	-	
UAM	93 ± 3	2.0 ± 0.2	2.0 ± 0.5	1.0 ± 0.7	traces	2.0 ± 0.7	
CIEMAT	92 ± 3	2 ± 1	2 ± 1	2 ± 1	traces	traces	traces

Silica minerals, carbonates and the other accessory minerals in the bentonite are included in coarse fractions. This is demostrated by the fact that the less than 2 μm fraction is fully composed of montmorillonite. Figure 1 shows the aspect of the diffractograms analysed. The less than 50 μm fraction shows the predominance of K-feldspar over plagioclase. This fact can not be detected in the bulk sample, probably due to the difficulties in the separate quantification of K-feldspar and plagioclase when they are in small quantities.

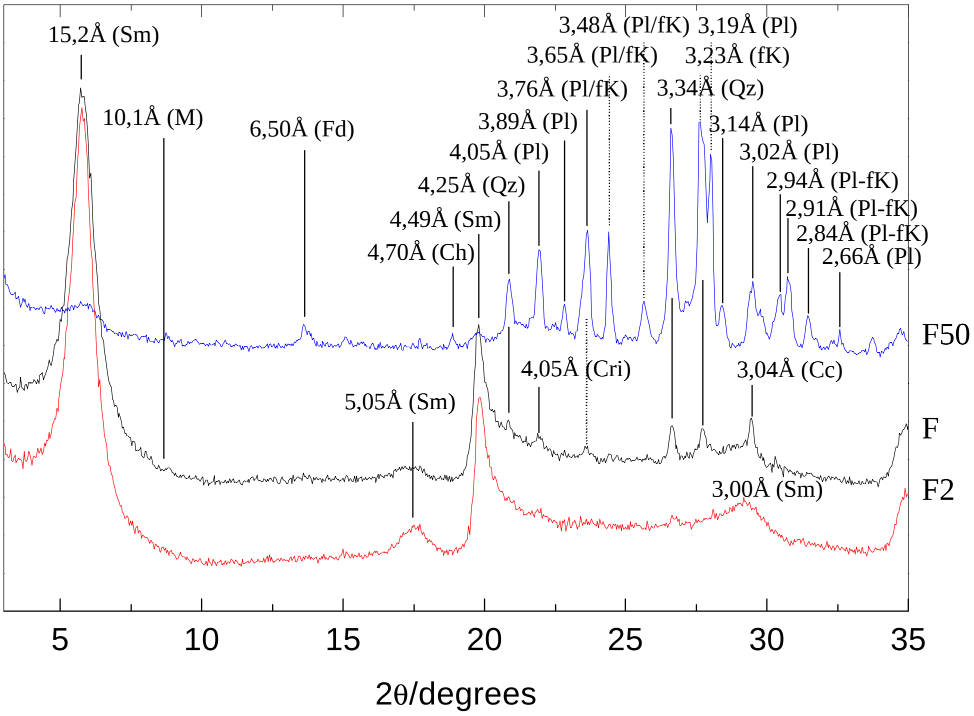

Figure 1: XRD random powder patterns of bulk sample (F), >50 µm size fraction (F50) and <2 µm size fraction (F2). Sm: smectite, Ch: chlorite, M: mica, Qz: quartz, Pl: plagioclase, fK: K-feldspar, Cc: calcite.

The XRD profile of the less than 2 µm fraction has been modelled by using the NEWMOD2© software (Reynolds 1985: Figure 2). The oriented etylene-glycol solvated profiles can be better simulated by considering the existence of a smectite crystallite population whose maximum size is of 10 layers coherently stacked perpendicular to the **c** dimension. A maximum distance of 4 layers free of defects is also taken into account (N=10, δ=4). Several models have been considered with the premise of the maintenance of the Valley/Peak (V/P) ratio. A 10 % of smectite/illite random interstratification (I/S R=0) is needed to fit properly the experimental diffractograms. This is in agreement with the data previously observed by Cuadros & Linares (1995) in a bentonite of the same deposit (S-2).

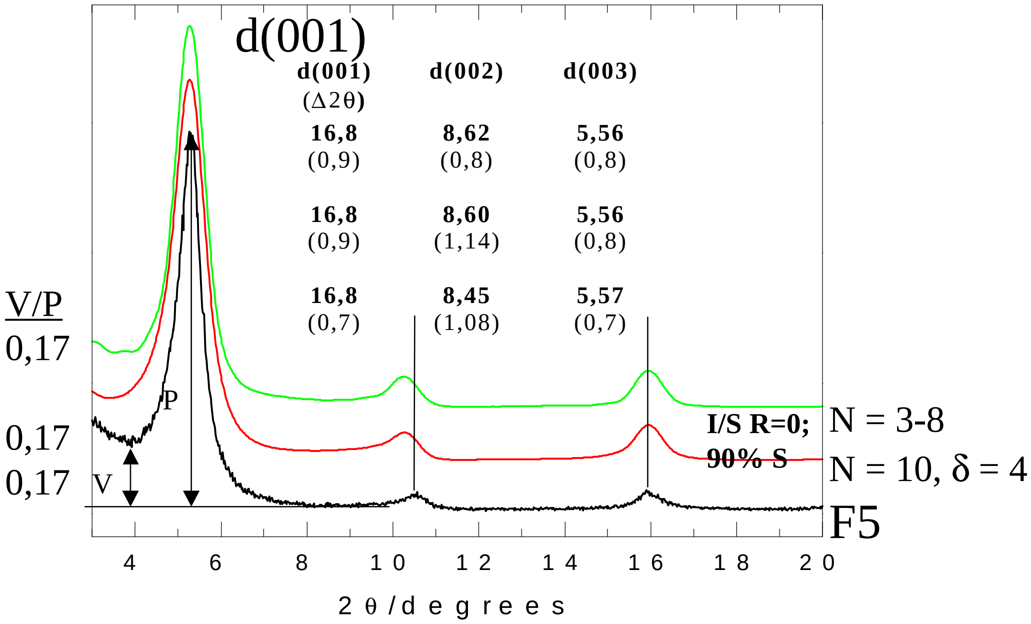

Figure 2: NEWMOD2© simulation of the <2µm Ca-homoionised ethylene-glycol solvated FEBEX clay. N = number of coherently stacked smectite layers. I/S R=0: random illite/smectite interstratified mineral. V/P: Valley/Peak ratio. F5: <0.5µm Ca^{2+} homoionised clay.

The mineralogical composition has been also observed and quantified by optical microscopy study of thin sections. Several compacted bentonite specimens were cut, freeze-dried and embedded in a LR-White acrylic resin (Kim et al. 1995). The textural aspect of the FEBEX bentonite under crossed polarised light is presented in a series of figures (Figure 3 to Figure 6).

The textural heterogenity itself is the main feature that can be described in the sample. The FEBEX bentonite is mainly composed of clay aggregates whose aspect ranges between dark isotropic low crystalline size ones (Figure 3) to those presenting preferred orientation and relatively large (sub-micrometric) crystals (Figure 4). The remaining elements of the texture are glassy materials, volcanic rock fragments and individual accessory minerals (quartz and feldspars). Calcite is usually present as esparitic crystals replacing feldspars (Figure 5), but it has been observed also as isolated micritic cements (Figure 6).

The mineralogical composition has been evaluated by a semiautomatic measure of the areas of the defined textural elements. This has been performed with the aid of the image analysis software LEICA QWIN®. Three thin sections of the untreated compacted clay were prepared. 32 microscope fields (enlargement x 256) were studied in each section, what has covered a 5% of the total area. An additional measurement with low magnification (x 68) has covered an 18 % of the bulk area and has been used to quantify the clay aggregates and the powder matrix. The results of these measurements can be seen in Table II.

Table II: Percent area quantification of textural elements in the FEBEX clay. Mean diameter.

	area (%)	mean equivalent diameter (μm)
clay aggregates	81.35 ± 18.71	462.9
quartz	0.43 ± 0.03	80.0
plagioclase	3.63 ± 0.04	108.5
feldspar	0.37 ± 0.02	77.7
opaques	0.16 ± 0.01	54.7
micas	0.057 ± 0.01	40.8
piroxene/amphiboles	0.70 ± 0.17	100.7
calcite	0.92 ± 0.09	75.6
volcanic glass	1.45 ± 0.06	87.2
rock fragments	1.23 ± 0.79	318.8
Matrix-voids (remaining area)	9.70	-

The percent area values have been recalculated to weight percent by assuming a direct correspondence between volume and area. The specific weight of the accessory minerals and the dry density of the compacted bentonite have been used to perform the volume-weight transformation. The results are shown in Table III. The calculated percentages are very similar to the XRD ones with the exception of those of feldspars. Optically, plagioclases are well distinguished by its size and aspect while K-feldspars are not. We have observed by SEM the frequent presence of polycrystalline aggregates of K-feldspar. Individual crystals have micrometric dimensions and it was not easy to identify these mineral grains. Another source of error in the K-feldspars quantification by XRD diffraction was the imprecise measurement of their low area peaks and the superposition of some peaks between K-feldspar and plagioclase (Andesine-Oligoclase).

Table III: Mineralogical composition (weight percentage): comparison between XRD and thin section data

Method	clay	cristobalite	quartz	K-feldspar	plagioclase	calcite
XRD	93	2	2	< 1	1	2
Thin section	91.3	--	0.7	0.6	5.8	1.5

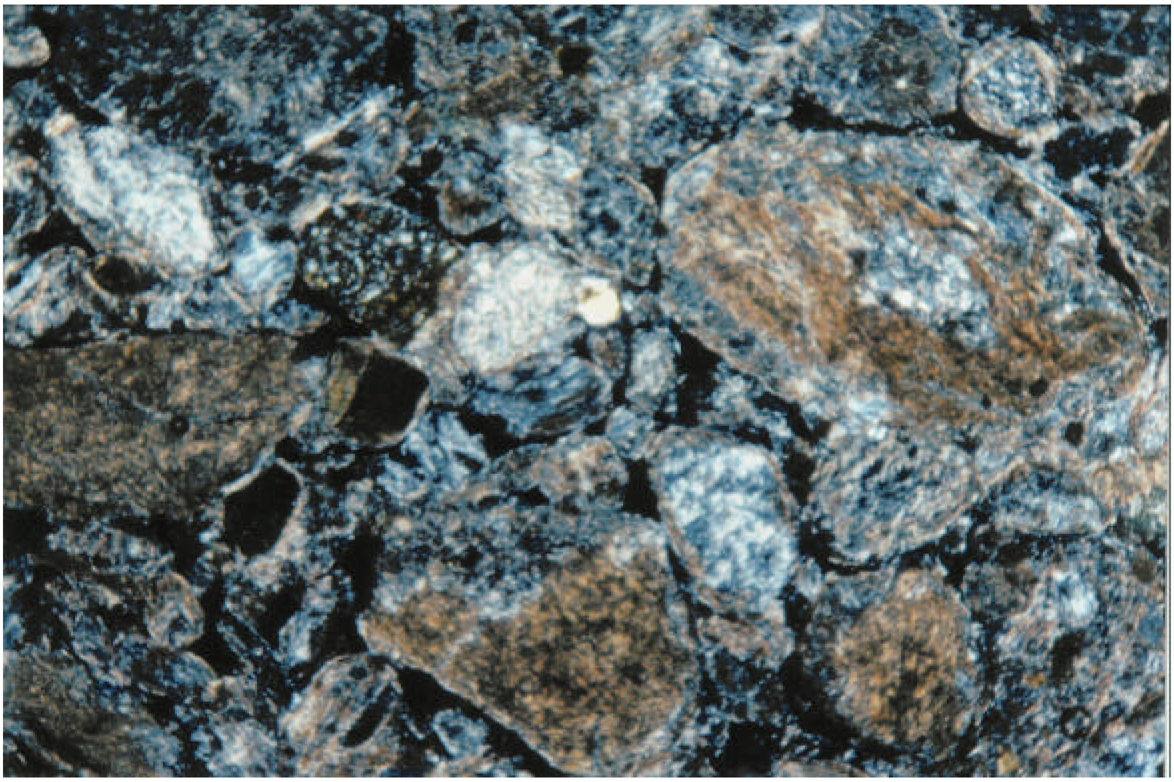

Figure 3: Bulk aspect of the Febex clay (enlargement x 37.5)

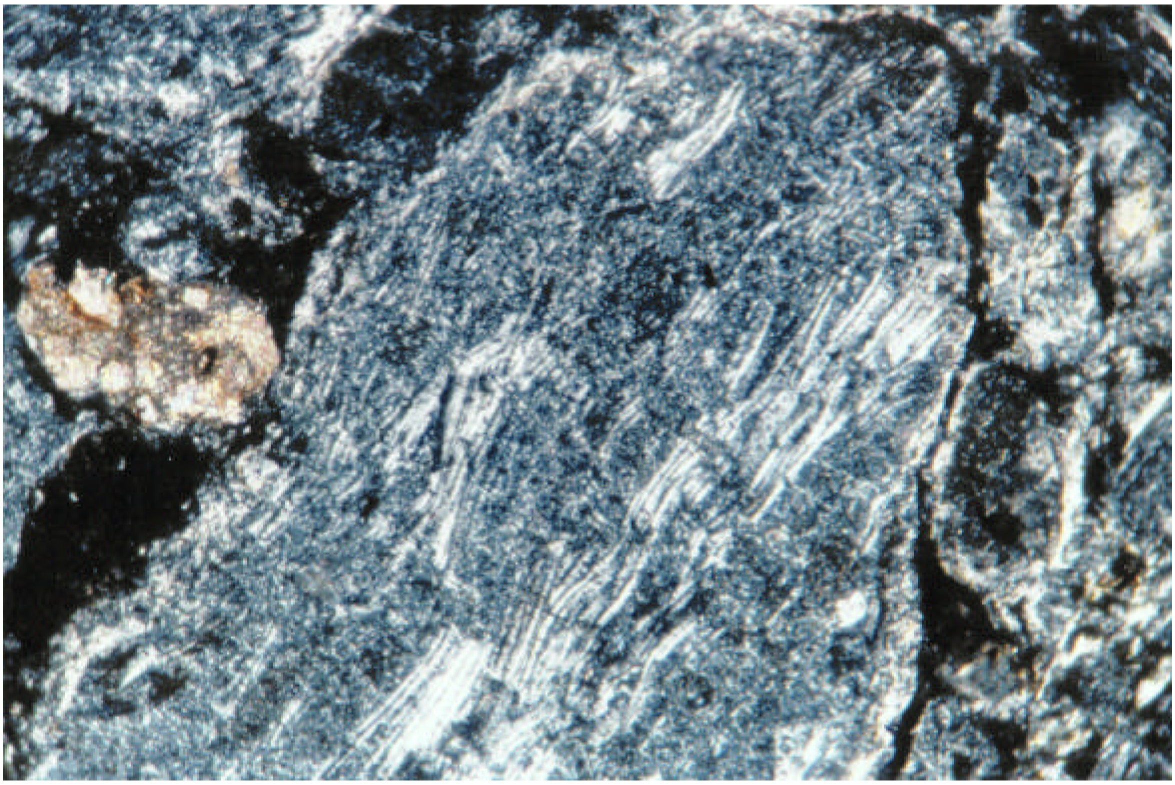

Figure 4: Detail of oriented clay (birefringent white lines) inside an aggregate (enlargement x 150)

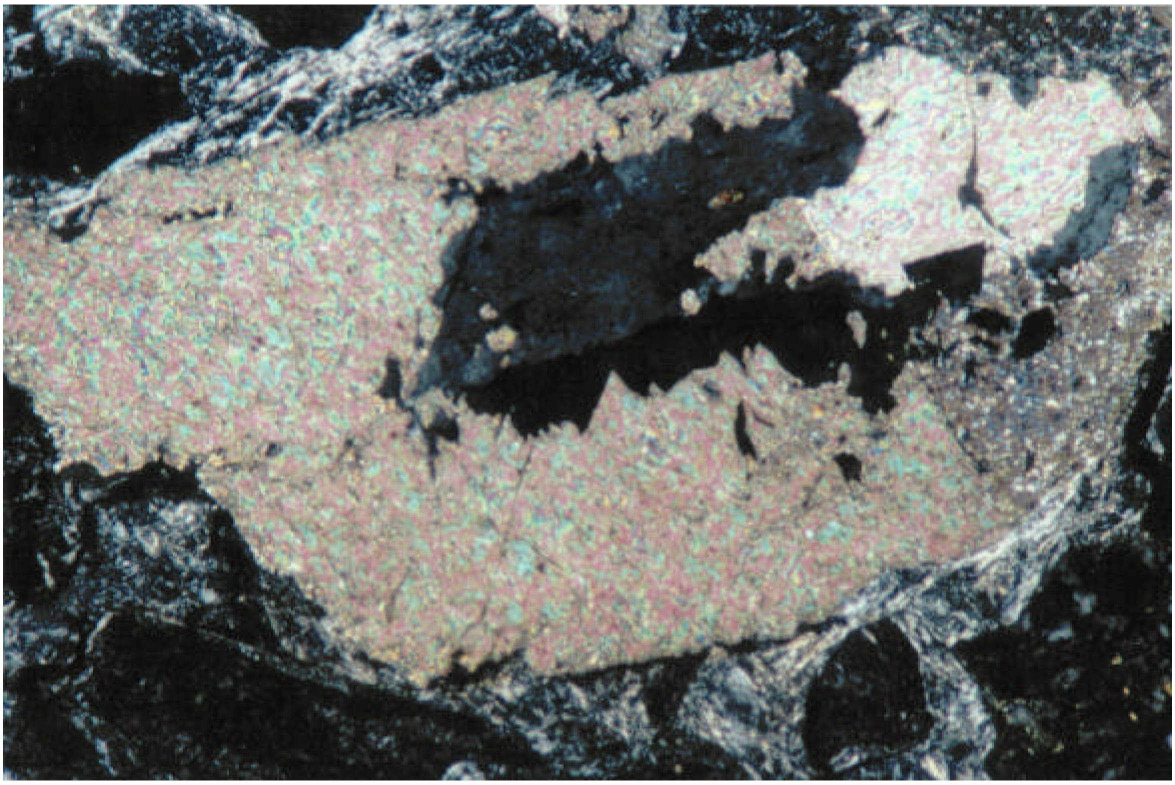

Figure 5: Sparitic calcite replacing a feldspar crystal (enlargement x 150)

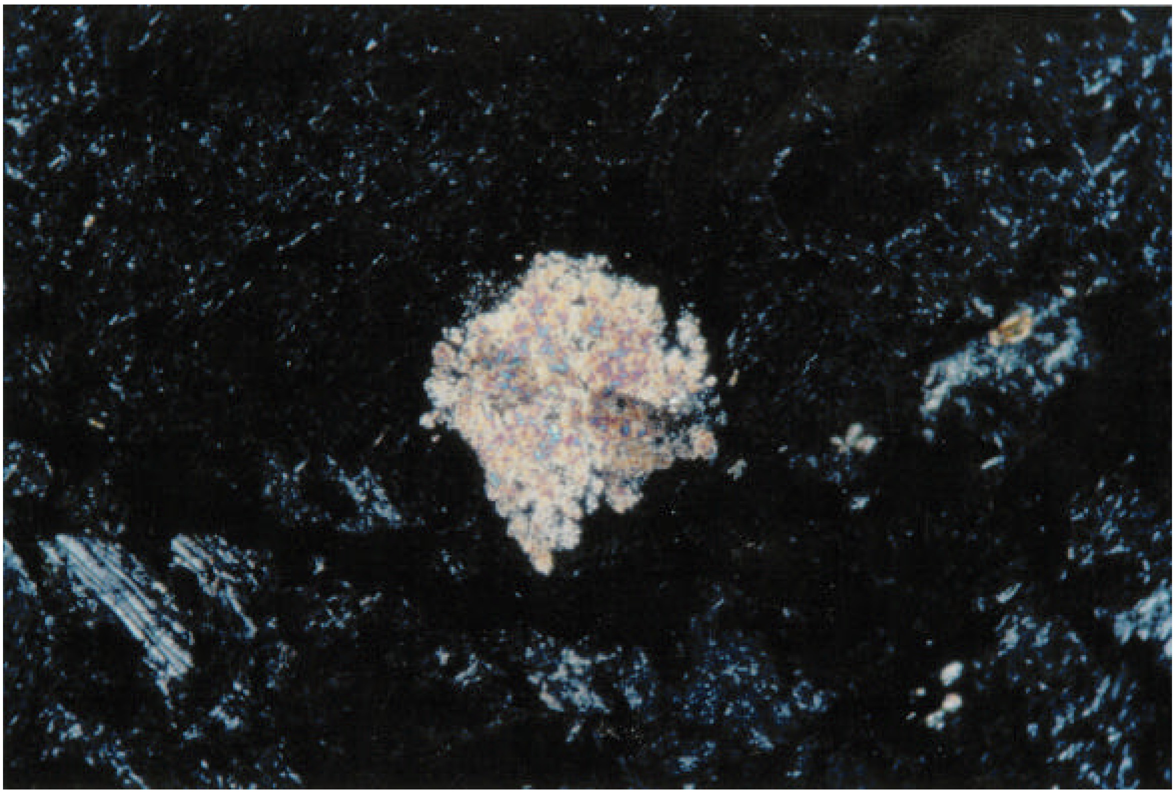

Figure 6: Polycrystalline micritic calcite inside a clay isotropic aggregate (enlargement x 150)

3.2. PHYSICOCHEMICAL PROPERTIES

The cation exchange capacity (CEC) of the FEBEX clay, determined as the sum of exchangeable cations displaced by 1M amonium acetate at pH 8, is of 102 ± 4 meq/100g (CIEMAT data), and the major exchangeable cations are: Ca (42 %), Mg (33 %), Na (23 %) and K (2 %). The Na/Mg exchange method at pH 7 used by UAM yielded 100±2 meq/100g. The N_2-BET surface (a_s) determined by UAM is 62±2 m^2/g. More than 80% of the pore space, measured by N_2 adsorption in powder samples, lies in a continuous range of the mesopore region (diameter 500-20 Å) with an average value of 91 Å. Table IV summarises the physicochemical properties that have been determined at UAM.

Table IV: Physico-chemical properties of the FEBEX clay (CEC: cation exchange capacity, SEC: sum of exchangeable cations)

specific N_2-BET surface (m^2/g)	**CEC** meq/100g	**exchangeable cations (meq/100g)**				
		Ca^{+2}	Mg^{+2}	Na^{+}	K^{+}	SEC
62 ± 2	100 ± 2	50 ± 2	39 ± 2	27 ± 1	1.8 ± 0.2	118
Distribution of pore sizes						
Size (Å)	<30	31-60	61-200	201-450	451-1500	
Percentage	8±2	11±4	20±4	25±4	36±8	

3.3. STRUCTURAL FORMULAE OF THE SMECTITE

The chemical composition of the less than 2 μm and less than 0.5 μm fractions of a Ca^{2+} homoionised clay has been determined at CIEMAT and UAM in order to calculate the structural formulae of the smectite (Table V). Both analyses show the montmorillonitic character of the clay and the remaining traces of K^+ that is fixed in the interlayer region (Illite-smectite (I/S) random interstratification). The lower values of K^+ and higher values of layer charge in the less than 0.5 μm formulae are due to the lower content of impurities.

Table V: Structural formulae

	tetrahedral sheet				octahedral sheet				interlayer		
	Si	Al	Tetrahed charge	(*) % charge	Al	Fe (+3)	Mg	Octahed charge	X^+	K^+	Layer charge
<0.5 μm	7.73	0.27	-0.27	21	2.70	0.39	0.85	1.03	1.20	0.09	1.30
<2 μm	7.83	0.17	-0.19	16	2.77	0.37	0.80	0.99	1.06	0.11	1.17

(*) % of tetrahedral charge related to total charge

3.4. ELEMENTS SOLUBILISED IN A 1/4 SOLID/WATER AQUEOUS EXTRACT

The chemical composition of an aqueous extract of bentonite/water ratio (b/w) of 1/4 is presented in Table VI. This data are the basis of the interpretation of transport phenomena that will be described below.

Table VI: Solubilised elements in the 1/4 bentonite/water aqueous extract. Concentrations are related to the dry mass of clay (mmol/100g, dried at 110ºC)

sample	**Cl**	**Br**	**HCO_3^-**	**SO_4**	**As**	**V**	**Na**	**K**	**Mg**	**Ca**
average	**2.03**	**$2.5\cdot10^{-3}$**	**1.56**	**1.84**	**$0.91\cdot10^{-3}$**	**$2.3\cdot10^{-4}$**	**6.04**	**0.062**	**0.146**	**0.067**
error	± 0.16	± 0.20	± 0.16	± 0.28	± 0.12	± 0.30	± 0.12	± 0.007	± 0.11	± 0.001
sample	**Sr**	**Ti**	**Mn**	**Fe**	**Ni**	**Cu**	**Zn**	**Y**	**pH**	
average	$5.8\cdot10^{-4}$	$4.2\cdot10^{-4}$	$1.1\cdot10^{-4}$	$1.3\cdot10^{-3}$	$9.2\cdot10^{-4}$	$0.82\cdot10^{-4}$	$0.91\cdot10^{-4}$	$1.0\cdot10^{-4}$	7.93	
Error (x 10^{-4})	± 0.6	± 0.8	± 0.2	± 0.6	± 12	± 0.2	± 0.3	± 0.2		

3.5. HYDROMECHANICAL PROPERTIES

For dry densities higher than 1.45 g/cm^3 the relationship between hydraulic conductivity (K, m/s) and dry density (ρ_d, g/cm^3) can be expressed by:

$$\log K = -3.0\ \rho_d - 8.6$$

This equation has been obtained from tests in which distilled water was used as permeant and the clay was directly compacted in the permeability cell. The variation of the experimental values with respect to this fitting is around 40 % (take into account that the permeability values are in the order of 10^{-13} m/s). The influence of the saturation water on the permeability values has been checked by performing tests in which either granitic or saline water were used as permeant (Figure 7). No differences have been found when granitic water is used, but with saline water, the values obtained are a 71 % higher than for distilled water and show a greater dispersion.

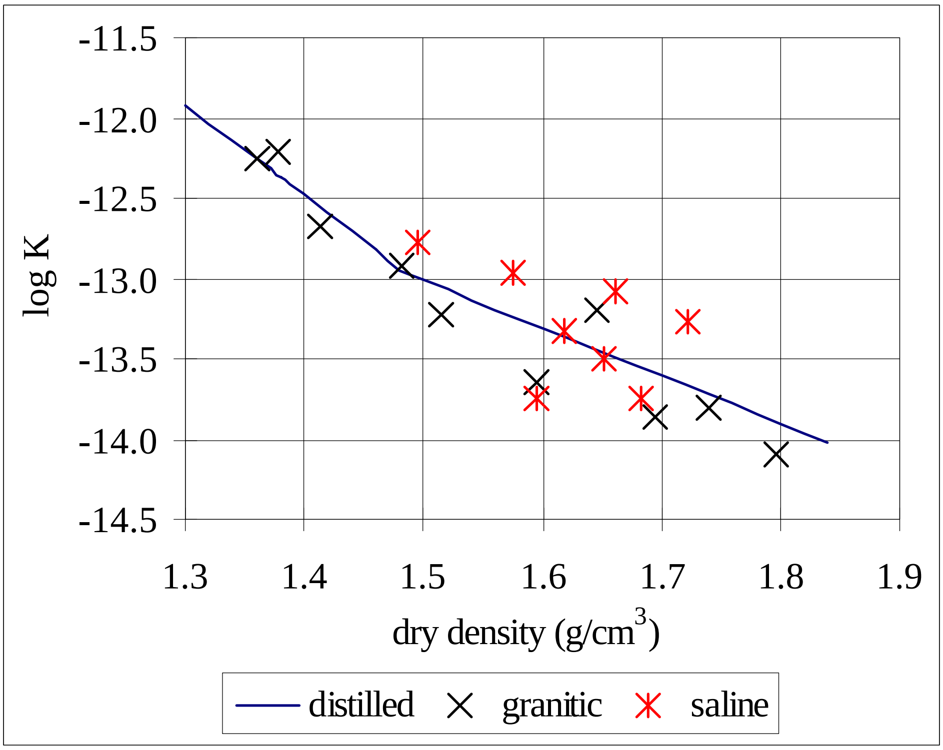

Figure 7. Influence of the saturation water on the hydraulic conductivity (K in m/s)

The swelling capacity of the bentonite has been determined on samples compacted to dry density of 1.60 g/cm^3 with the water content at equilibrium with the laboratory conditions (around 14%), saturated in oedometers under different vertical loads. Both granitic and saline water have been used as saturation liquid. The values obtained are represented in Figure 8, where the strain percentage is calculated as the increase of height with respect to the initial height of the sample, the negative values indicating swelling strains. The fittings obtained for both kinds of water are also shown in the figure. A slightly higher swelling capacity has been observed in samples saturated with saline water.

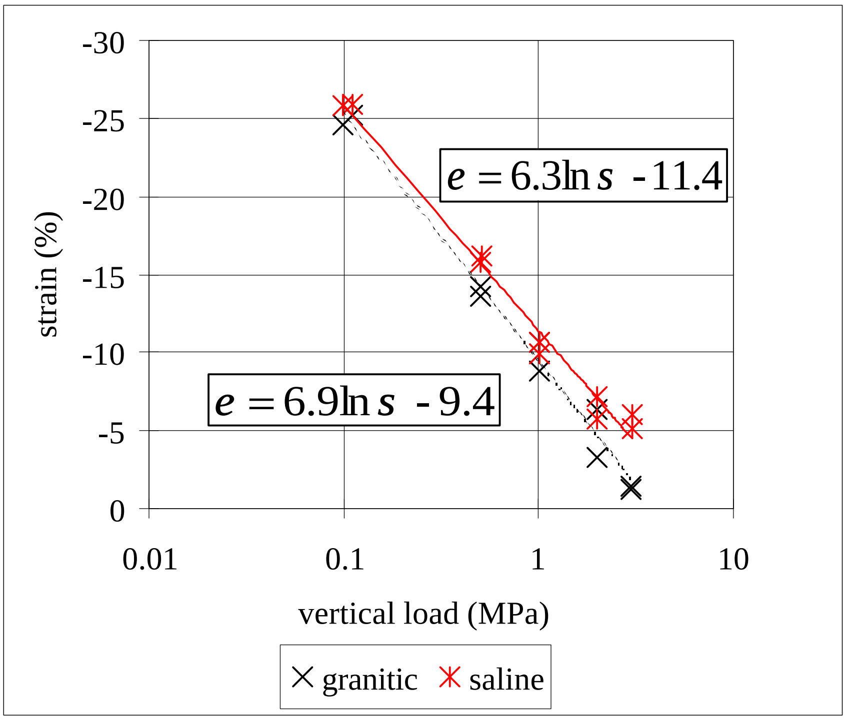

Figure 8. Strain (ε) measured upon saturation with different water under a given vertical load (σ)

4. THERMO-HYDRAULIC (TH) TREATMENT

The tests have been performed in hermetic cells in which a compacted block of bentonite is hydrated on the top while a thermal gradient is applied from the bottom.

The body of the cell is made out of Teflon, although an external steel cylinder prevents its deformation swelling (Figure 9). A plane heater constitutes the bottom of the cell and on the top of the cell a chamber allows the circulation of water at a controlled temperature, lower than that of the heater. A hydration channel crosses the upper chamber and allows the hydration of the sample through a stainless steel sinter. The water is injected under a pressure of 1.1 MPa.

The clay, with its water content at equilibrium with the laboratory conditions, is uniaxially compacted outside the cell to a dry density of 1.65 g/cm^3. The specimen obtained is placed in the cell, where the dry density of the bentonite is of 1.59 g/cm^3. The specimen is only 2.5 cm long and 5.0 cm diameter, what implies that saturation is reached in a few days. This allows the performance of a large number of tests of different duration and conditions.

Two different thermal gradients are examined, in order to ascertain the effect of temperature in the observed processes: a high gradient, between 100 and 60 °C (16 °C/cm) to simulate regions closer to the container, and a lower gradient, between 60 and 35 °C (10 °C/cm), to simulate zones near the host rock. Although in the text, the experiments are referred to as “high gradient” (A) or “low gradient” (B) ones, in fact, the main difference between both is the range of temperatures involved, much higher in the case of the “high gradient” experiments.

The influence of the chemistry of the hydration water on the processes observed is verified by using two types of water: granitic (G), simulating the conditions of the outer part of the barrier, or saline (S), which simulates the situation in the internal part of the barrier, where water is loaded with the ionic species dissolved during its inward movement (Table VII). The last one has a chemical composition similar to that of the bentonite interstitial water (Fernández & Cuevas 1997), but simplified to include only the major elements.

The duration of the experiments is related to the saturation time. The time needed for saturation (t) has been verified previously, and it is of 16 days for the experiments at low temperature and of 10 days for the experiments at high temperature. The increase of hydraulic conductivity with temperature accounts for this difference. The tests have different duration related to the saturation time: t1/4, t1/2, t1, t2, and t5. That is, t1/4 means 2.5 days for the experiments performed at high temperature and 4 days for the experiments performed at low temperature, t1 means 10 days for the experiments performed at high temperature and 16 days for the experiments performed at low temperature, t5 means 50 days for the experiments performed at high temperature and 80 days for the experiments performed at low temperature, etc.

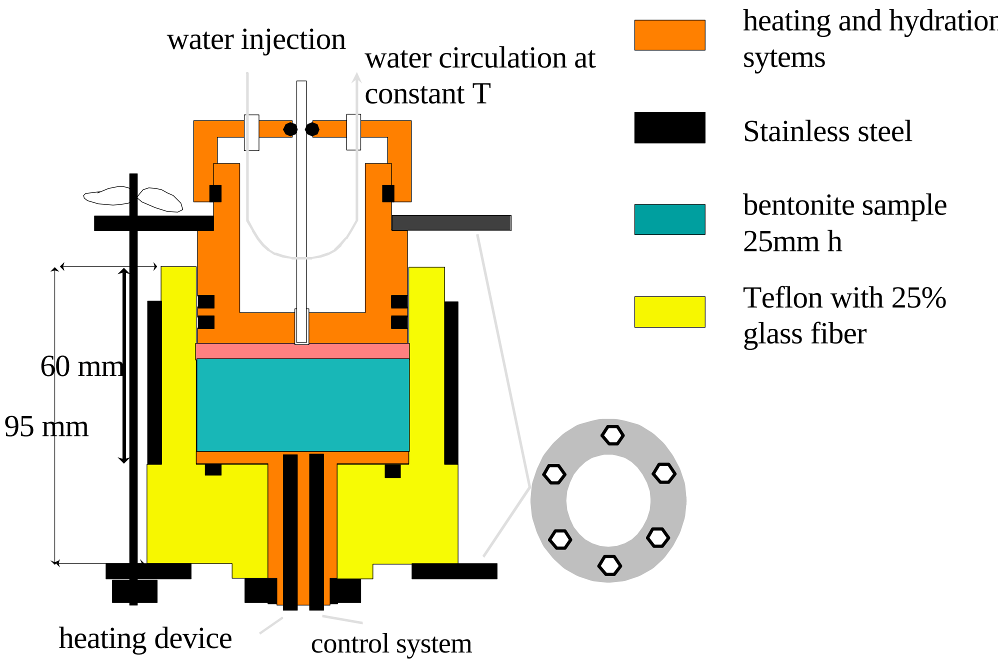

Figure 9. Schematic design of the small cells for thermo-hydraulic tests

Table VII. Chemical composition of the water used in the tests

Element (mmol/l)	Granitic	Saline
Cl^-	0.37	100
SO_4^{2-}	0.15	15
HCO_3^-	2.36	
Mg^{2+}	0.39	15
Ca^{2+}	1.12	10
Na^+	0.48	80
K^+	0.026	
pH	8.3	7

Figure 10 shows the rate of water uptake in the experiments. A total of 12-13 cm^3 are needed to reach full saturation. The initial fast rate of hydration makes that almost a 90% of the water intake capacity enters the clay at half the time measured for complete saturation.

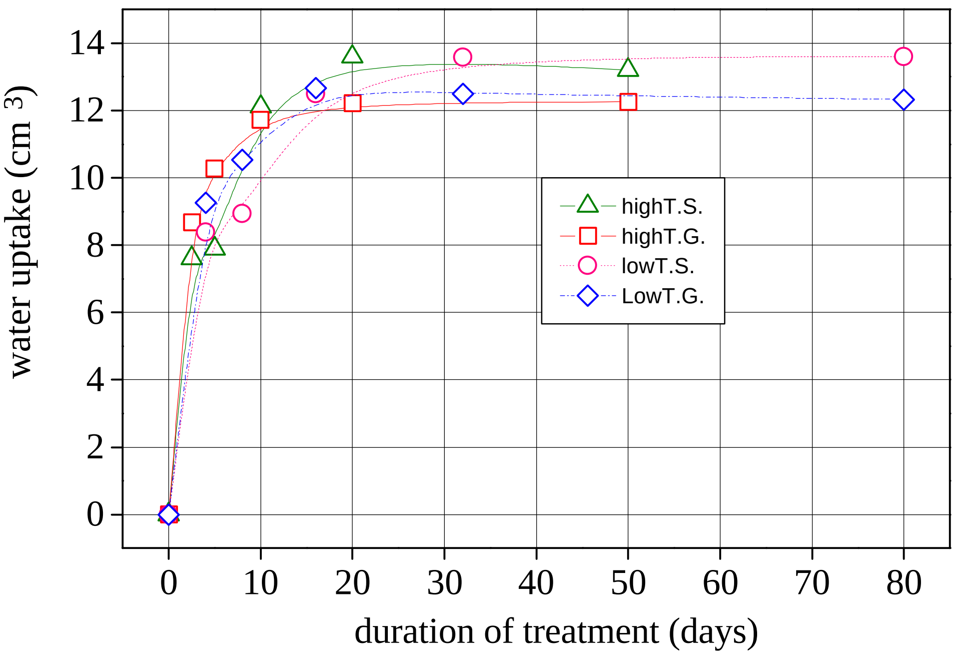

Figure 10. Water uptake rate under high and low thermal gradient conditions. S: saline water; G: granitic water

Four tests of the same characteristics (duration, kind of water and thermal gradient) have been performed. In one of them a geochemical characterisation of the clay in different sections parallel to the heating front is carried out once the TH experiment is dismantled. This is the "transport" experiment (T). The concentration of ions in an aqueous extract, the exchange complex, the specific surface and, in some cases, the mineralogy, are determined. The other tests are dedicated to check the influence of heating and/or hydration on the retention and hydro-mechanical properties of the clay and the fabric/microstructure modifications. These are the "fabric" (F), "swelling" (H) and "permeability" (P) tests. The particular methods and results will be presented in the following sections. Some of the tests have been duplicated or even triplicated.

5. GEOCHEMISTRY

5.1. TIME DEPENDENT DISTRIBUTION OF SOLUBLE SALTS

At the end of each experiment the clay was sliced in 5 sections of 0.5 cm height. In these samples, the concentration of major ions and pH were determined in a 1/4 bentonite/water aqueous extract by the methods described in ENRESA (1998). The distribution of exchangeable cations and the total cation exchange capacity (CEC) were also determined by means of the ammonium acetate method and by Na/Mg exchange, respectively (Thomas 1982).

Figure 11 and Figure 12 compare the distribution of several ions at three different stages in which the time for complete water saturation (t) is considered as the time scale unit for both temperature gradients. The ions Cl^-, SO_4^{2-}, Na^+ and Mg^{2+} have been chosen because they represent the different behaviours that have been observed among the different ions analysed. The two parallel lines that are drawn in the figures represent the average ion concentration in the untreated clay (F) and the average concentration that should be reached with the salt input of the solution uptake in the saline water experiments (S).

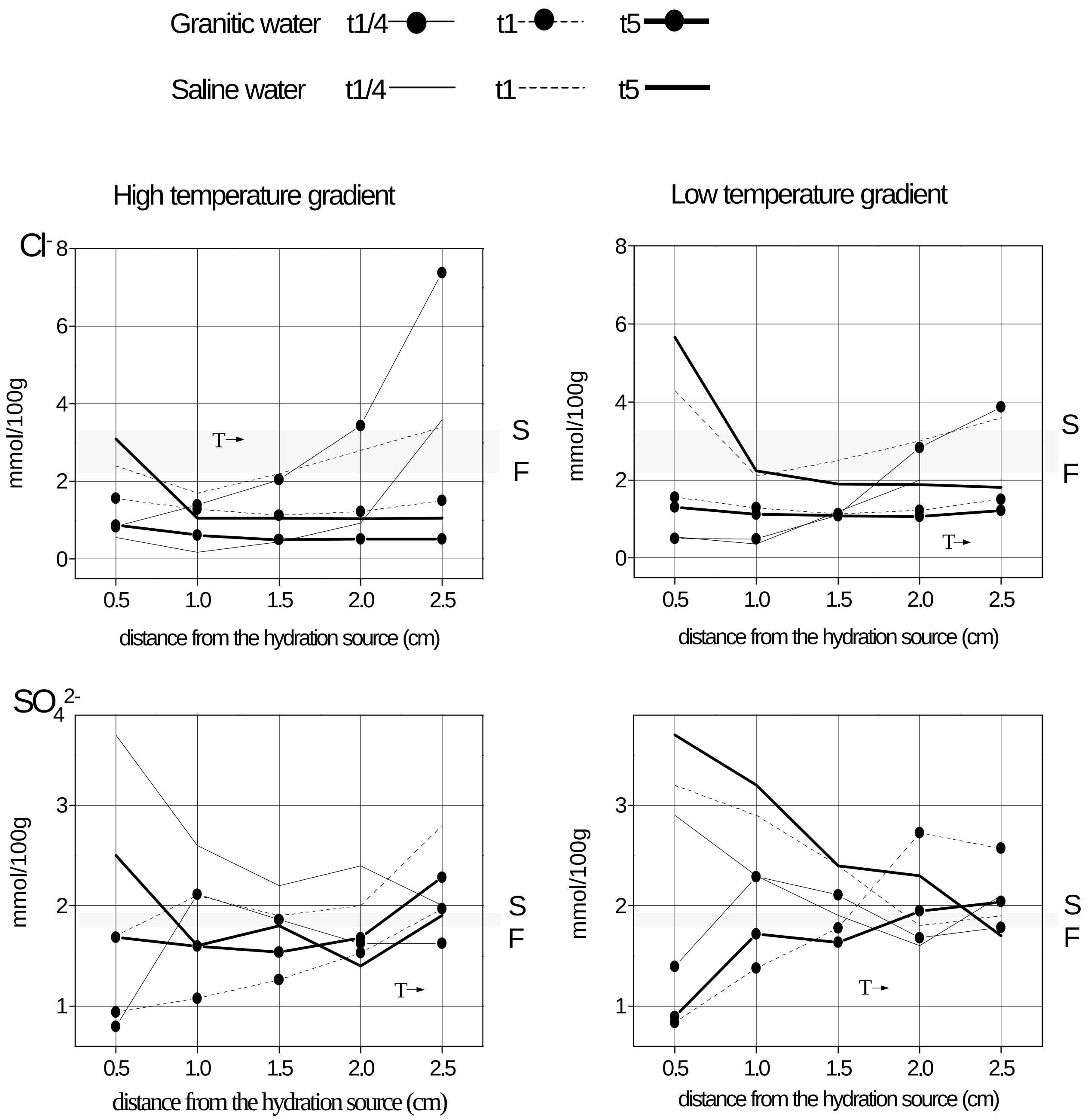

Figure 11. Time dependent distribution of the concentration of selected ions. Lines marked with solid circles are the granitic water experiments. F: ion concentration in the untreated clay calculated from the aqueous extract;. S: average calculated ion concentration for F plus the saline water input; t: time for full saturation

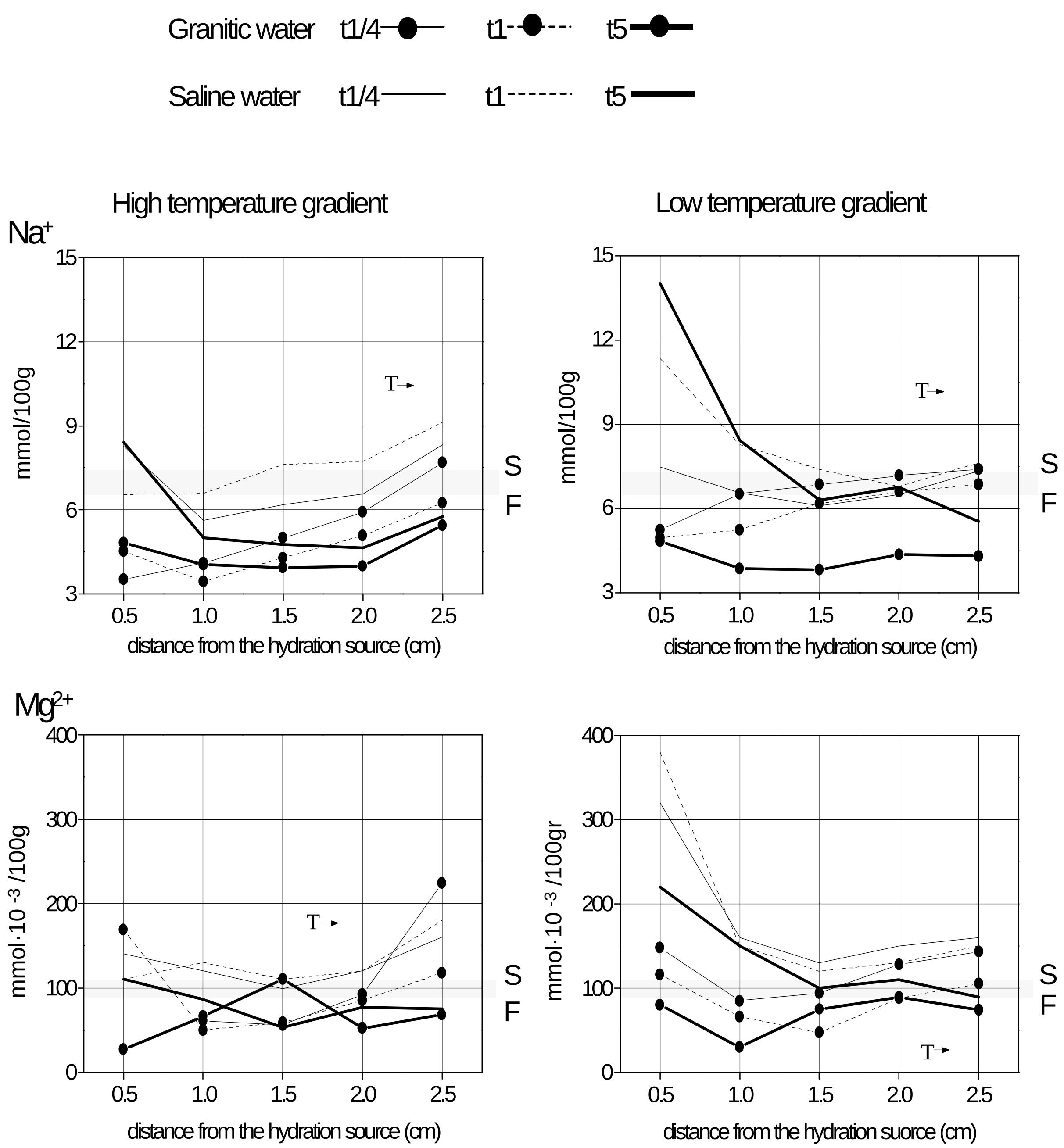

Figure 12. Time dependent distribution of the concentration of selected ions. Lines marked with solid circles are the granitic water experiments. F: ion concentration in the untreated clay calculated from the aqueous extract;. S: average calculated ion concentration for F plus the saline water input; t: time for full saturation

At the beginning of hydration, there is an advective transport of ions linked to the movement of water. It is mostly the Cl^- and Br^- anions that move and reach higher concentrations towards the heater, especially in the high temperature experiments. Na^+, Ca^{2+}, Mg^{2+} and Sr^{2+} follow roughly the same trend, but K^+ remains at a constant low level (less than 0.1 mmol/100g). When saturation is reached, the concentration gradient of Cl^- has virtually disappeared, but a slightly higher concentration of Na^+ remains in the heater zone, either when granitic or saline water are injected under high thermal gradient. In general, these effects are less traceable at low temperature.

The effect of injecting saline water yielded complex results. These tests show similar or even lower Cl^- concentrations at the beginning of hydration than the tests performed with granitic water. From the first hydration stages, Cl^- has lower concentrations than the expected ones from the calculated input considering the amount of saline water injected (Figure 13). This can be explained by ion exclusion at the bentonite interface.

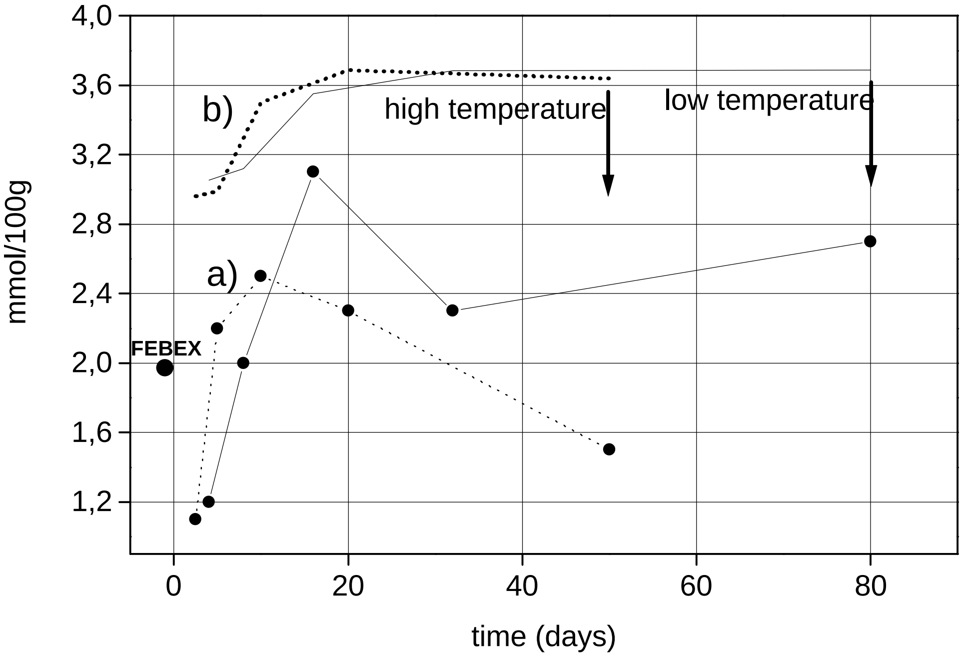

Figure 13: Time dependent concentration of chloride in the saline water tests. a) experimental data, b) data calculated by adding the FEBEX concentration to the solute loaded water inflow during the experiment

After full saturation in the experiments with saline water, a generalised maximum of salt concentration develops at the water-bentonite interface. This effect is more pronounced in the tests performed at low temperature, and constitutes a significant difference with respect to the tests performed with granitic water, especially in the sulphate behaviour. This ion is mainly depleted near the hydration source in the experiments performed with granitic water, but concentrates at this interface when saline water is used. The cause for the sulphate concentration is still not clear, but could be explained either as a contamination coming from the porous sinter material, as a specific reaction involving sulphur species in the clay or as an increase in the concentration of the water injected caused by its evaporation at the inlet (hermetic system failure). The contamination from the porous sinter has been tested and, although possible, remains within the uncertainty of data. The source of sulphate is not continuous, as the sulphate concentration in the aqueous extracts does not increase with time (Figure 14). This fact prevents us to consider the sinter alteration as the main cause for sulphate contamination and also the evaporation at the water source-bentonite interface (closed system failure).

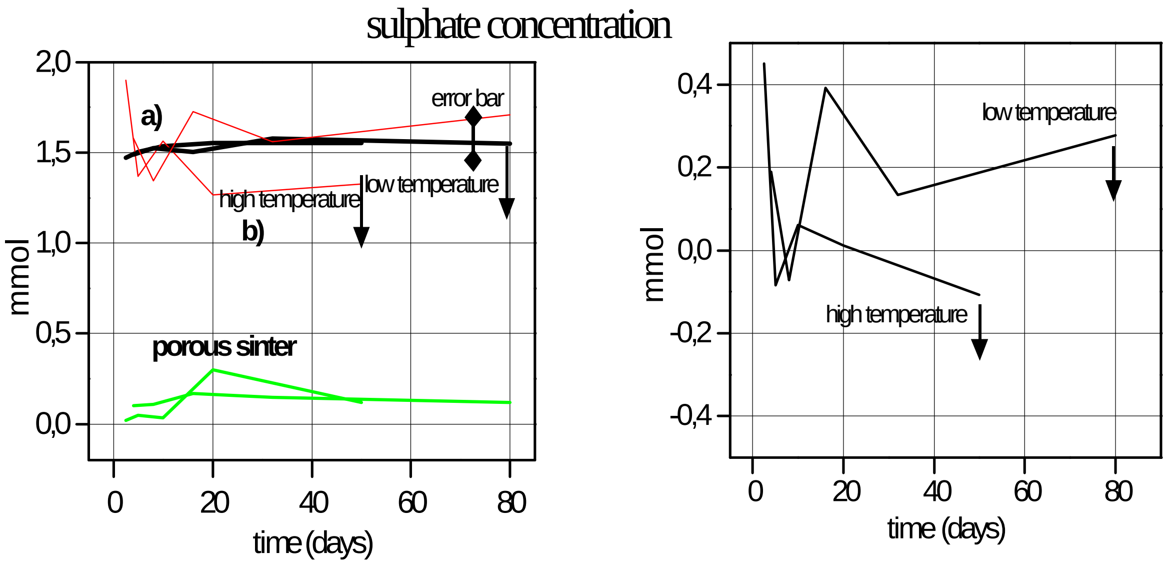

Figure 14: Sulphate mass balance in the saline tests. a) total sum of moles for a perfect close system: calculated input plus bentonite content, b) experimental data. The graph on the left is the porous sinter content plus the experimental data subtracted from a.

Nevertheless, the increase of concentration in the external water with respect to the pore water in the compacted clay has been observed by several authors (Kharaka & Berry 1974, Muurinen & Lehikoinen 1997). It is explained in terms of the high degree of overlapping in the Gouy–Chapman double layer within the smectite layers, what lowers dramatically the pore water anion concentration and promote the salt migration outside the clay platelets and the inhibition of anion transport by surface diffusion mechanisms.

From the plots on Figure 11 and Figure 12, it can be inferred that mainly the Na^+ ion counteracts the charge balance, although the remaining major divalent cations rise also their concentrations near the hydration surface.

There exists a group of “mobile” elements that are associated to the main salt gradients represented by the sodium-chloride advective front or the sulphate anomalies at the water source: Ca, Mg, Sr, Br and, in the saline case, K^+.

During the advective stage (1/4 to 1/2 t) a maximum gradient of concentration is generated for the elements that concentrates in the heater zone. This gradient at t1/2 (5 days or 8 days for the high or low temperature, respectively) has been considered as t=0 for the diffusion phenomena observed towards the hydration source. Taken into account the concentration data for the three slices more close to the heater, an apparent diffusion coefficient for some “mobile” ions has been calculated using the Fick’s law solution described by Madsen and Kahr (1993) or Idemitsu et al. (1997):

$$\log C(x) = K - \frac{0.1086}{D_a \times t} x^2$$

Where, x^2 is the distance from the concentration source, t is the time, and C is the concentration of the ion calculated as the moles of ion dissolved in the bulk water content of the sample. The results obtained for the ions which fitted the straight line represented by the diffusion solution are in Table VIII. The order of magnitude (10^{-10} to 10^{-11} m^2/s) and the increase with temperature are in agreement with the reported data for compacted bentonites (Madsen, 1998). Chloride data are within 1 order of magnitude lower than its reported mobility in free water (2 x 10^{-9} m^2/s; Robinson and Stokes 1959). Hence, the data reflects a very high mobility of this ion through the compacted bentonite before and after saturation.

Table VIII contains also the data calculated for As. This element concentrates in the hydration end at the beginning of the test, in opposition to the NaCl behaviour, and diffuses with time. For the set of trace elements that have been analysed, in addition to Sr and Br, is the only element that dissolves from the bentonite. Cu and Zn are suspected to be introduced by their leaching from the metallic components of the experimental system and Mn, Fe, V, Ti, Ni and Y are clearly related to the presence of a fine colloidal fraction in the filtrated solutions (Cuevas & Martín 1998, 1999). A suggestion that arises from the As behaviour is that this element could be a “self-tracer” solute in the bentonite. Its concentration as soluble anion would be related to changes in redox potential and will be readily precipitated by sulphide species at Eh lower than 0.3V and near neutral pH.

Table VIII Apparent diffusion coeficients (m^2/s)

	granitic water		saline water	
Ion	high gradient	low gradient	high gradient	low gradient
Cl^-	$2.95\cdot10^{-10}$	$8.0\cdot10^{-11}$	$2.0\cdot10^{-10}$	$2.8\cdot10^{-11}$
Na^+	$1.3\cdot10^{-10}$	$5.0\cdot10^{-11}$	$1.1\cdot10^{-10}$	$7.2\cdot10^{-11}$
Br^-	$3.4\cdot10^{-11}$	$5.2\cdot10^{-11}$	$3.7\cdot10^{-11}$	$3.65\cdot10^{-11}$
AsO_4^{3-}	$1.1\cdot10^{-10}$	$1.87\cdot10^{-10}$	$7.9\cdot10^{-11}$	$2.9\cdot10^{-11}$

With the exception of the effects registered at the slice that represents the hydration interface, salt concentration is well below that of the untreated clay average value (F) with respect to chloride, and remains constant for sulphate within the uncertainty of data, in both the saline and granitic experiments. These results represent evidences for anion exclusion and migration of salts outside the bentonite probe. Figure 15 shows how the total salt concentration (ΣM^+) decreases significantly with time in the experiments performed with granitic water. Similar results are achieved in the experiments performed with saline water under high temperature, taking into account that the initial salt input in these tests is higher.

The most interesting fact involving transport phenomena is the rapid movement of chloride towards the heater, caused by the entering of either saline or granitic water in the bentonite. This implies some degree of ion exclusion. In a homogeneous saturated smectitic clay, anion transport will be inhibited in the absence of a net advective flow, a fact that could be supported looking at the sulphate behaviour. From our point of view, the rapid decrease of chloride concentration after the bentonite hydration can be explained by the existence of preferential passages between or through the primary clay macro-aggregates that remain active even when bentonite is saturated. In this sense, relatively continuous 1 mm thin fissures have been observed in the bentonite near the heater zone with fine coatings or iron oxides, an evidence of a solute free transport (Cuevas et al. 1999).

The low mobility of SO_4^{2-} can be explained only in terms of solubility, if we think that the external water (macro-mesopores) moving through these passages will be more concentrated than the interlayer pore water (micropores). Flow-through experiments reported by Kharaka & Berry (1974) do not show a retardation of sulphate transport with respect to chloride in montmorillonite under injection pressures of 60 MPa.

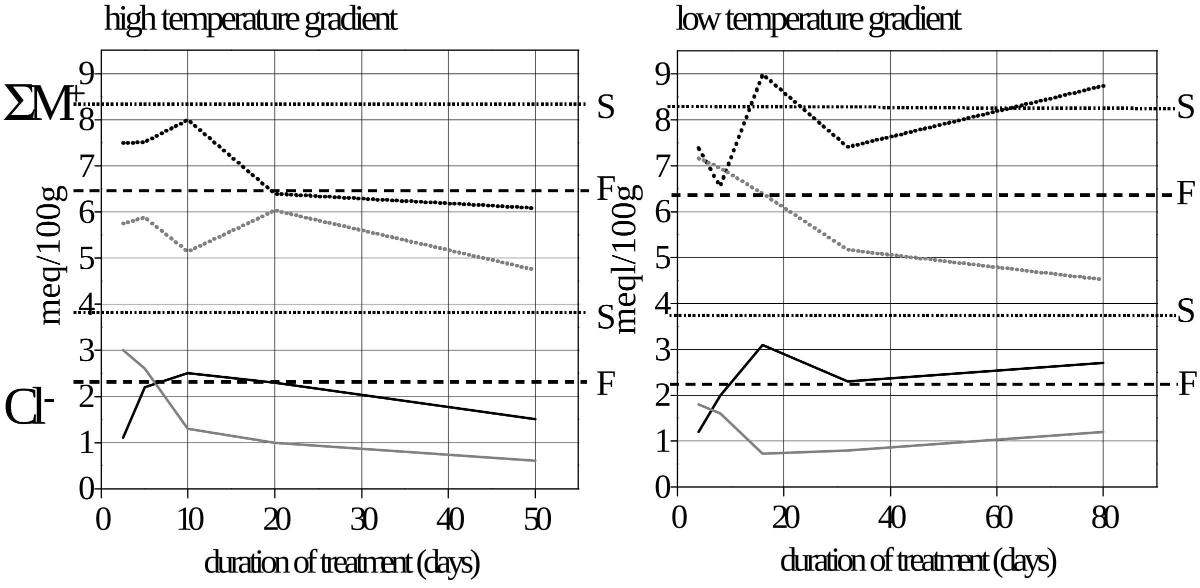

Figure 15. Evolution of global salinity during the experiments. ΣM^+: sum of equivalents of dissolved cations (global salinity). Black lines: saline water experiments. Grey lines: granitic water experiments. F and S are the same reference values quoted in Figure 11 and Figure 12

5.2. THE SOLID PHASE: MINERALOGICAL AND CHEMICAL RESULTS

The other geochemical parameters that have been determined show a high degree of invariance. Bicarbonates and pH are rather constant in all the experiments. These parameters are buffered from calcite equilibrium and stay at values of 1.5 ± 0.3 mmol/100g and 8.0 ± 0.2.

Calcite is present in all the samples, and has been detected in slightly higher amounts near the heater zone in some experiments by XRD diffraction measures (Figure 16). In fact, there were no clear trends on calcite evolution detected by means of XRD. The scattering of the data is close to the experimental threshold (Table IX). The bulk mineralogy is virtually the same as initial FEBEX bentonite as can be deduced viewing the aspect of the diffractograms.

Table X summarises the average values of pH and cation exchange capacity after the TH treatment for the different experiments. The amount of exchange capacity seems to increase in the low temperature experiments with respect to the high temperature ones, but all the values are very close to those of the untreated sample. This is in agreement with the non-significant mineralogical transformations detected by XRD regarding the smectitic predominant component.

The structural formulae calculations for the long treatments can be added in proof for the previous statements (Table XI). All the treated samples show a reduction in octahedral charge when compared with the FEBEX montmorillonite, but there are no significant differences among them. The layer charge is slightly higher in the granitic tests but there is no relation with temperature as indicated by the CEC data.

Finally, the constancy of atomic proportions of the fixed K^+ in the smectite indicates that the I/S interstratification is not changing during the tests. As the process of illitization is time/temperature dependent we have estimated the percentage of illite in the I/S random interstratified phase by means of XRD modelling in the slices closest to the heater and in the longer tests.

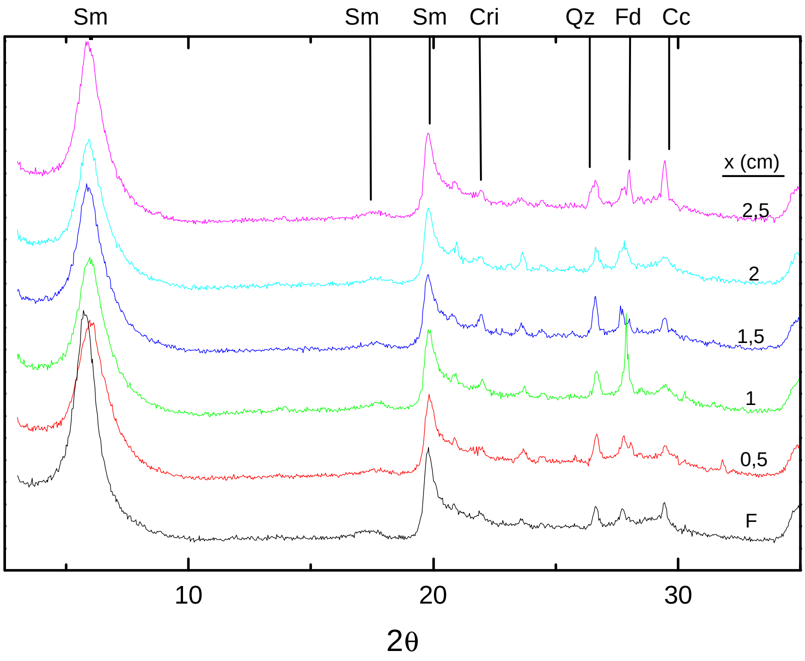

Figure 16: XRD diffractograms for the saline low temperature gradient test (80 days). Sm: Smectite; Cri: Cristobalite; Q: Quartz; F: Feldspars; Cc: Calcite; F: FEBEX; x: distance to the hydration source.

Table IX: Mineralogical composition (weight percentage) of the long term treated samples (50 or 80 days; high T or low T). The values are average data from the 5 slices analysed in each experiment

Sample	Smectite	Cristobalite	Quartz	K-Feldspar	Plagioclase	Calcite
low T granitic	92.9±1.2	1.4±0.2	1.4±0.2	1.3±0.4	1.7±1.3	1.3±0.4
high T granitic	93.0±0.9	1.3±0.1	1.4±0.2	1.6±0.5	0.8±0.4	1.8±0.8
low T saline	94.3±0.8	1.1±0.3	1.6±0.3	0.9±0.1	0.8±0.4	1.4±0.5
high T saline	94.5±0.7	1.0±0.2	1.3±0.3	0.98±0.4	1.1±0.6	1.1±0.3

Table X. Average values and standard deviation of pH and exchange capacity properties

WATER	GRANDIENT	pH	CEC (meq/100g)	EXCHANGEABLE CATIONS (meq/100g)			
				Mg^{2+}	Ca^{2+}	Na^+	K^+
Granitic	high	8.1±0.2	96±3	35±2	50±2	26±1	1.6±0.2
Granitic	low	8.1±0.2	104±4	36±2	50±2	27±1	1.6±0.2
Saline	high	7.9±0.1	97±3	38±3	49±2	28±1	1.7±0.2
Saline	low	7.9±0.1	101±2	40±3	50±3	32±2	1.8±0.3

Table XI: Average data for the structural formulae in the long experiments. δ: standard deviation in the formula calculation from the <0.5µm fraction for the 5 slices extracted and analysed in each experiment. CHT: tetrahedral charge. CHO: octahedral charge.

	tetrahedral layer			octahedral layer					interlayer		
sample	Si	Al CHT	% CHT	Al	Fe (+3)	Mg	Ti	CHO	X^+	K^+	layer charge
low T granitic	7.70	0.30	27.4	2.70	0.41	0.91	0.018	0.80	1.01	0.10	1.11
δ	$8\cdot10^{-3}$	$8\cdot10^{-3}$	0.8	$8\cdot10^{-3}$	$4\cdot10^{-3}$	0.02	$4\cdot10^{-3}$	0.03	0.01	0	0.01
high T granitic	7.70	0.30	26.1	2.68	0.41	0.90	0.020	0.83	1.05	0.10	1.15
δ	0.02	0.02	0.9	0.01	$8\cdot10^{-3}$	0.01	0	0.04	0.03	$4\cdot10^{-3}$	0.04
low T saline	7.68	0.32	28.5	2.71	0.42	0.89	0.014	0.80	1.00	0.11	1.12
δ	0.02	0.02	2	0.01	$5\cdot10^{-3}$	0.01	$5\cdot10^{-3}$	0.02	0.02	0.02	0.02
high T saline	7.67	0.33	30.0	2.72	0.41	0.89	0.012	0.78	0.99	0.10	1.10
δ	0.06	0.05	6	0.02	0.01	0.03	$4\cdot10^{-3}$	0.07	0.01	$9\cdot10^{-3}$	0.02

Table XII: Percentage of illite in I/S interstratified phases. Data form the slices near the heater in the long tests

sample	valley/peak ratio	% Illite in I/S
F5GB55	0.17	7
F5GA55	0.18	9
F5SB55	0.16	7
F5SA55	0.18	8
FEBEX	0.16	7

6. MICROSTRUCTURE

6.1. BET SURFACE AND PORE SIZE DISTRIBUTION

BET N_2 adsorption measurements have been performed at the end of the experiments of duration t1/2, t and t5. This parameter represents the external surface (a_s) without the interlayer pore space. Thus, it is a measure of the available area for solute transport in the compacted bentonite and of the degree of coherent stacking of smectite platelets (Sposito 1992). Figure 17 shows the average values for the five slices determined in each test. The experiments performed with granitic water present minor changes in the specific surface. There is only a significant decrease (of 10 m^2/g) in the slice in contact with the heater at the beginning of hydration, but this effect disappears when the bentonite becomes saturated. In the tests performed with saline water there is a generalised decrease of specific surface at the beginning of hydration, but it increases again with time, specially at high temperature. This increase can be attributed to a progressive lost in the number of stacked layers, what implies a disaggregation of the smectite flakes.

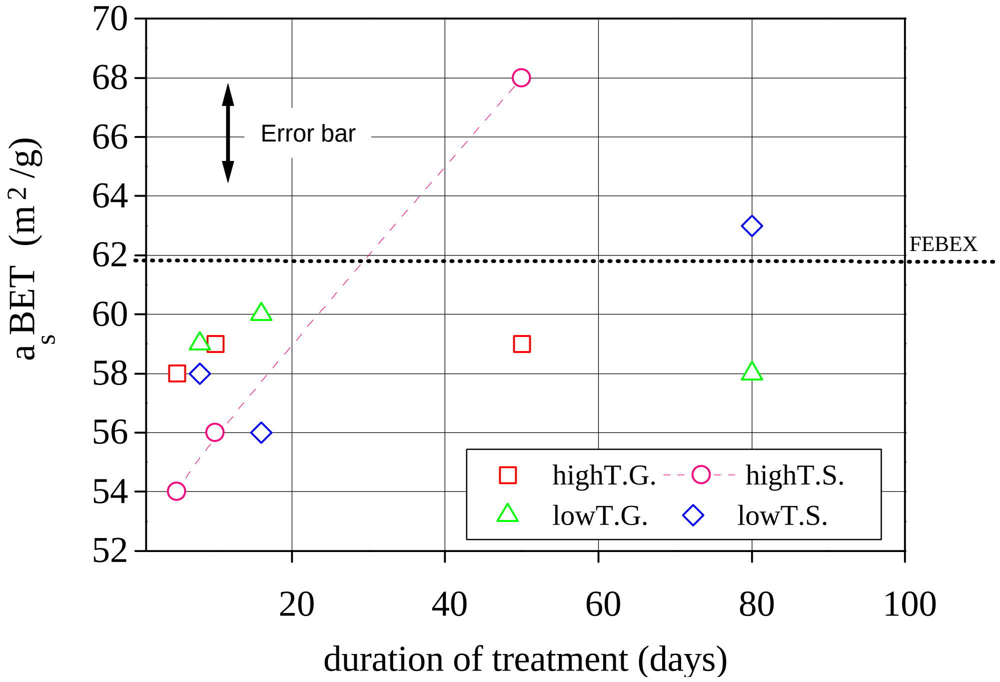

Figure 17 Average surface area (a_s) as a function of the duration of TH treatment. high T, low T: high or low temperature. G, S: Granitic or saline water. FEBEX: value for the untreated clay

The relatively constant value of specific surface area is in agreement with the constancy in the pore size distribution. Figure 18 presents the pore size distribution at the end of the longer experiments (50 days) performed under high thermal gradient, and the values for the untreated clay (FEBEX). The slightly higher values of the average pore diameter in the treated clay are not significant. The relative error in the mean pore diameter is ±10 Å.

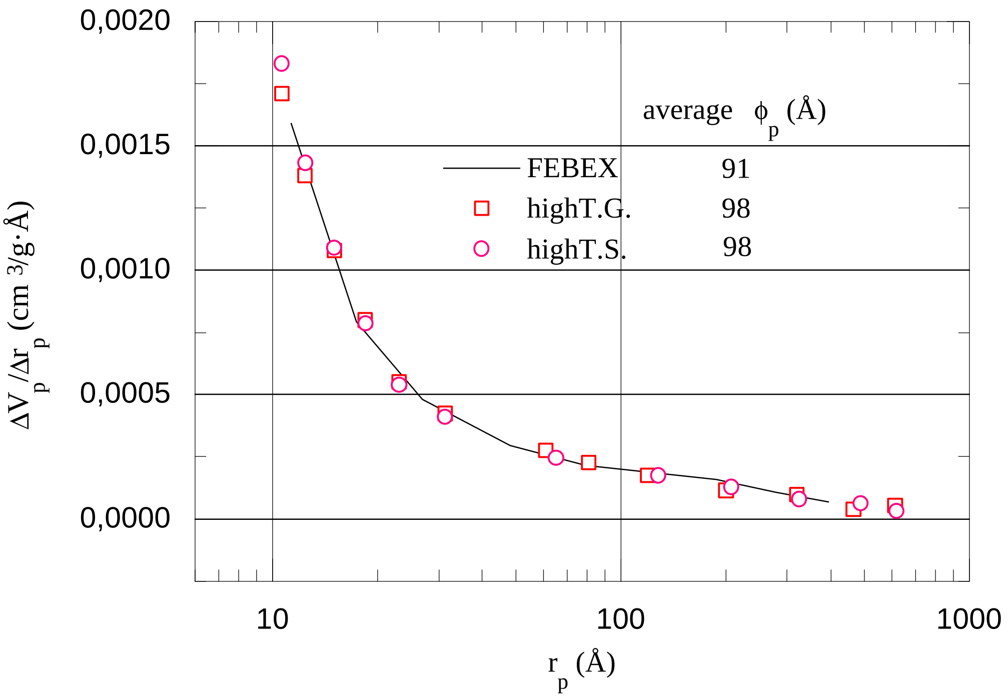

Figure 18. Pore size distribution by N_2 adsorption before (FEBEX) and after 50 days of TH treatment at high temperature. ϕ_p : pore diameter; r_p: pore radius; G, S: granitic or saline water; $\Delta V_p/\Delta r_p$: pore volume/pore radius increment ratio

6.2. OPTICAL MICROSCOPY

The treated samples have been prepared as thin sections for polarising optical microscopy observation. The samples are embedded in an acrylic resin (LR-White) after liofilisation, following a procedure modified from Kim et al. (1996). The detailed optical characterisation is presented in a topical report in which is described the complete optical microscopy determinations (Cuevas et al. 1999).

6.2.1. Microstructural observations

The comparison between the microstructural characteristics of the initial compacted bentonite and the hydrated one can be seen in Figure 19 and Figure 20. The fabric is similar in both samples. The shape and aspect of the aggregate entities are the same. Logically, the optically detectable porosity has disappeared.

With regard to the solute transport discussion, some micro-fissures (1mm length) inside the clayish macroaggregates and in the bentonite matrix have been identified. They are stained by iron oxides, mainly in the heater zones at complete saturation (Figure 21). This fact, and the existence of fine grained calcite around rigid microcrystals or vitreous volcanic rock fragments should be studied in greater detail, in relation to the transport of "mobile" porewater in the bentonite (Figure 22).

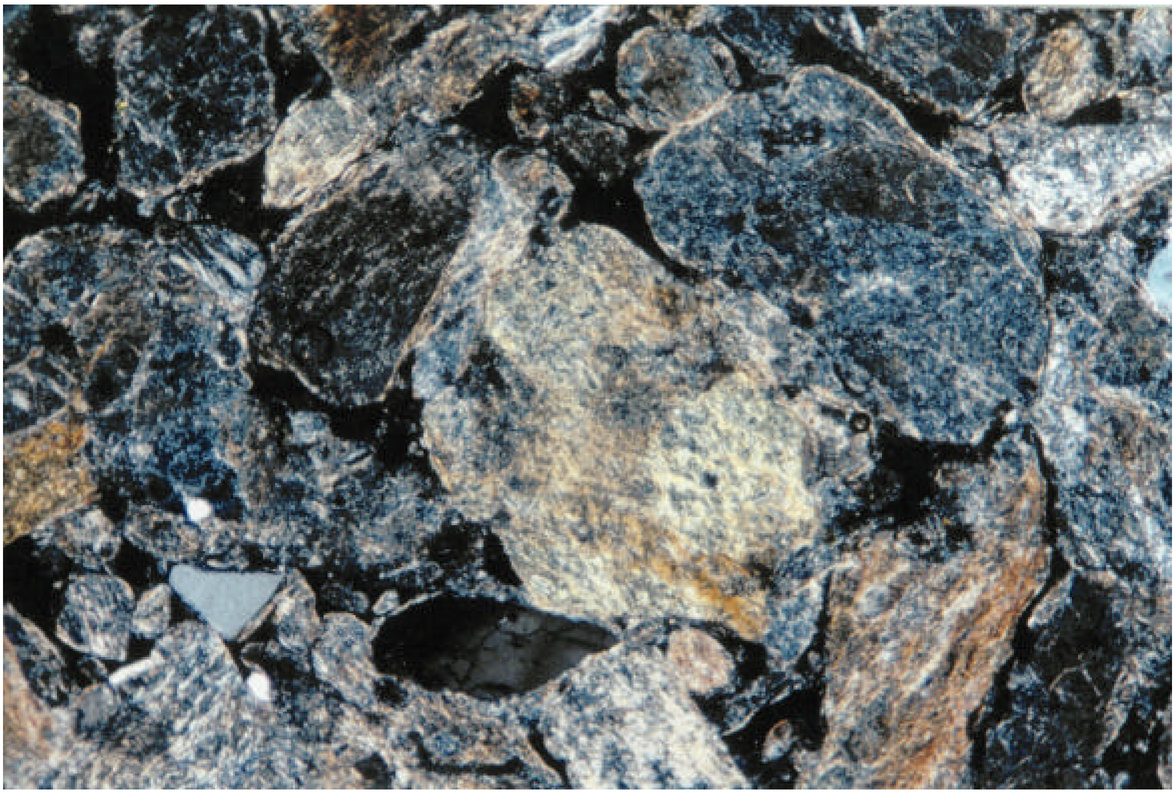

Figure 19: Febex clay: unsaturated aspect (enlargement x 37.5)

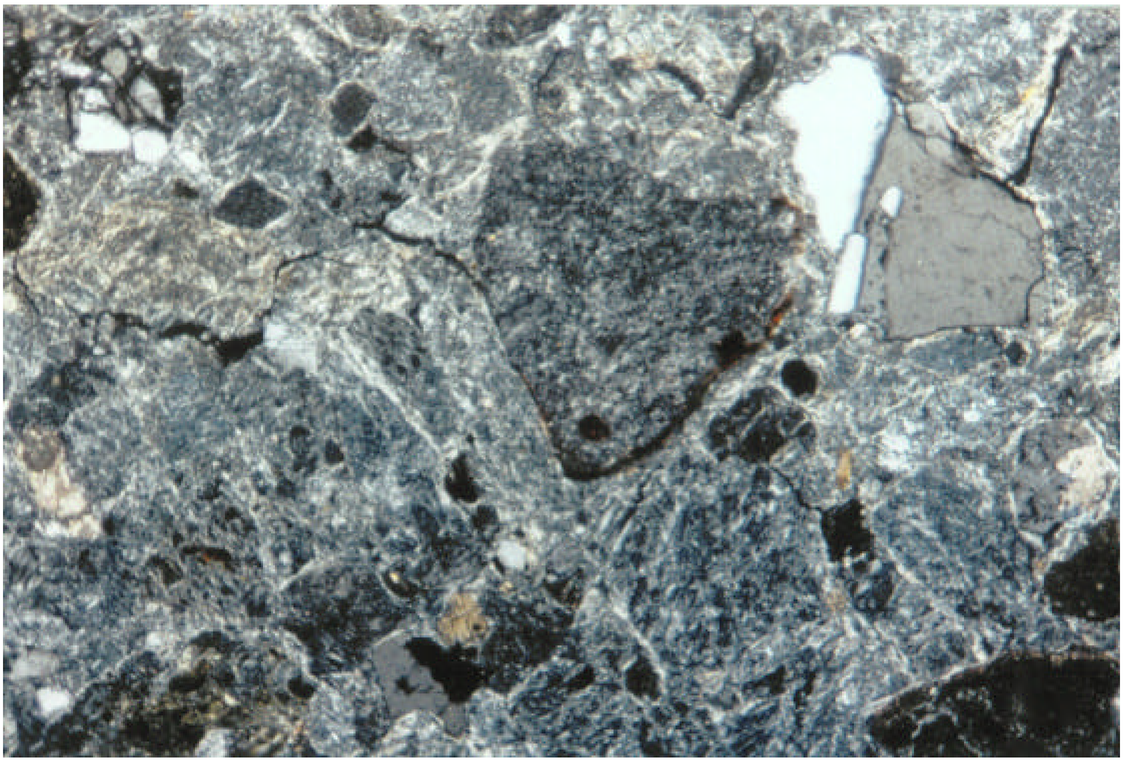

Figure 20: Hydrated soldered fabric after 50 days of thermo-hydraulic treatment with granitic water under high temperature gradient conditions (enlargement x 37.5)

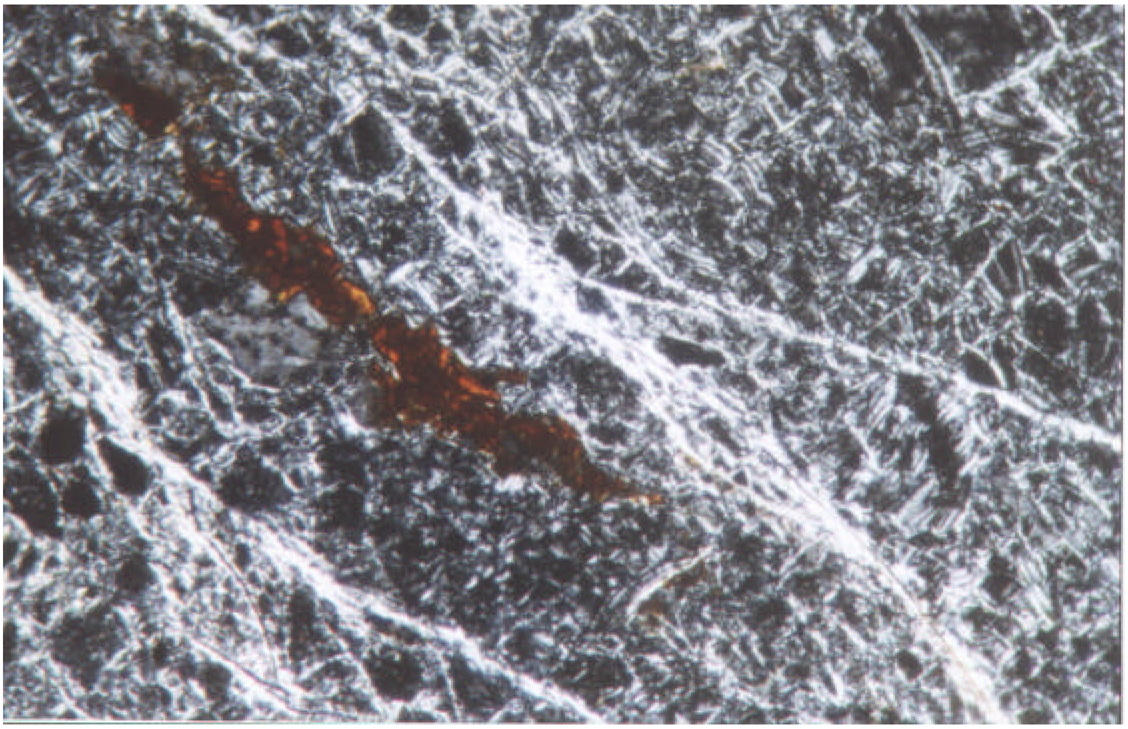

Figure 21: Fissural pattern in a birefringent clay aggregate: staining of iron oxides near the heater zone in a 10 days high temperature gradient test with granitic water (enlargement x 150)

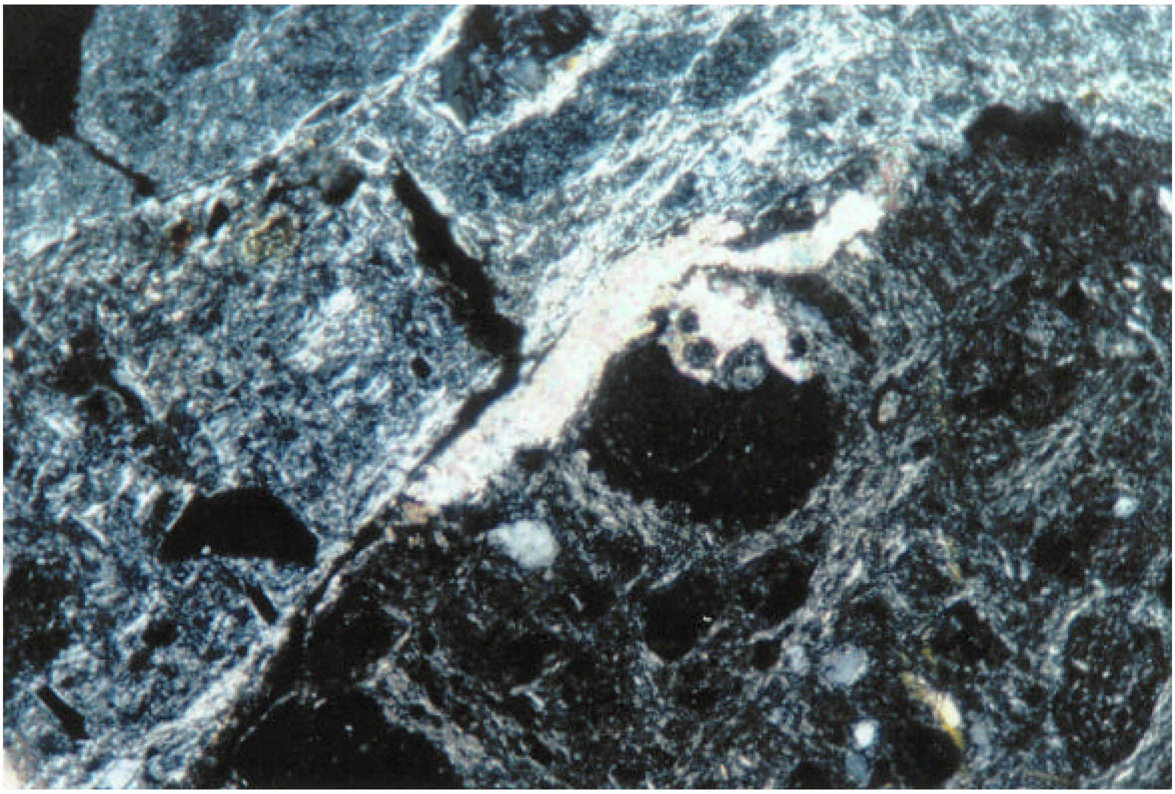

Figure 22: Micritic calcite at the glassy rock fragment- isotropic clay aggregate interface (enlargement 150)

6.2.2. Birefringence measurements

We have observed the increase in clay orientation around rigid and plastic interfaces (microcrystals and clay aggregates) in the bentonite. This can be distinguished by the increase of white tones at these interfaces, i.e. increase of birefringence (Figure 23). Random orientations produce the predominance of grey tones while preferred orientations outline black and white colours (Dudoignon & Pantet 1998).

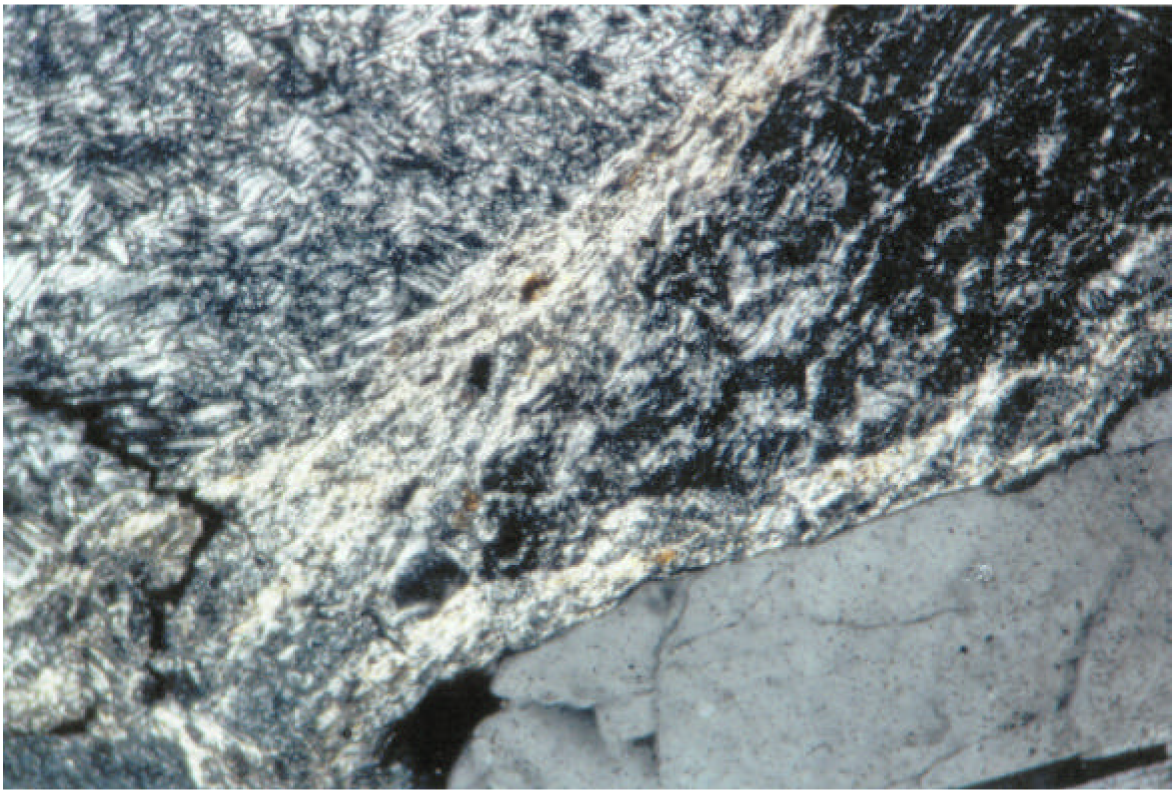

Figure 23: Detail of the aspect of oriented “bright clay” between the interface of two clay aggregates (enlargement x 150)

We have quantified the distribution of the different levels of grey (256 levels) in the five sections parallel to the temperature gradient in the tests performed with granitic water of duration t1 and t5, with the aid of the image analysis software LEICA-WIN©. Figure 24 shows the spatial distribution of the percentage of area with near-white tones (245-255 interval) taken from the average of five distinct measures with different rotating angles in each slide. There is an increase of white tones towards the hydration zone in the 10-day test and a generalised increase in the 50-day test. This effect is related to the redistribution of low density matrix materials that flow under the compression due to swelling of higher density macroaggregates. A microstructural rearrangement possibly occurs also inside the aggregates, as they have a significant influence in the whole birefringence analysis. This effect is not so clearly observed at low temperatures or under saline conditions, where the relative changes between the different slices of bentonite are not very important.

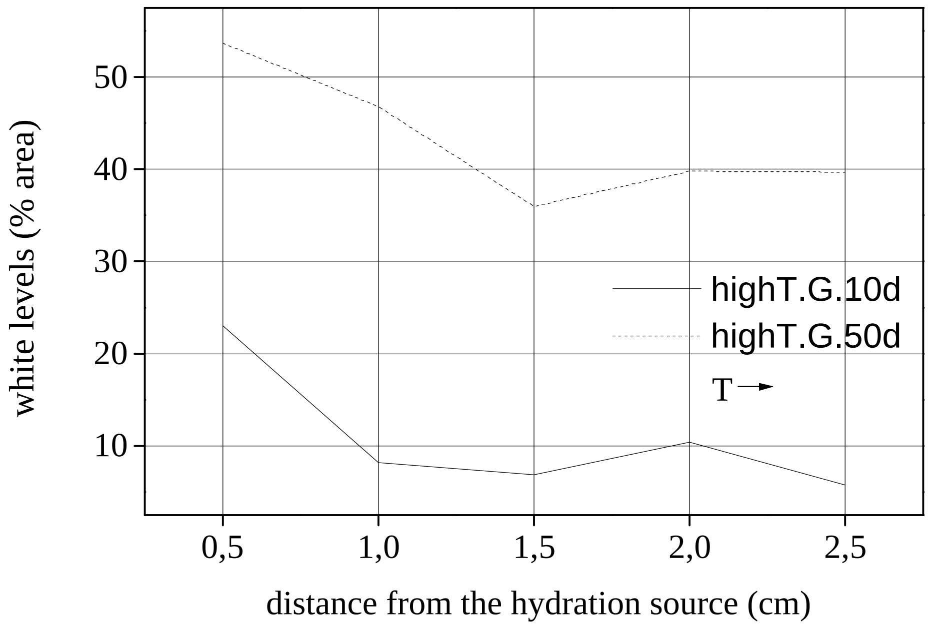

Figure 24. Relative white tone area quantified by image analysis in optical microscopy of the clay after TH treatment with granitic water at high temperature during 10 and 50 days

This assay of quantification has to be developed more deeply in order to understand the relationship between hydration and preferred orientation in the clay matrix. Figure 25 is a sketch of the microstructural evolution of the bentonite when it is hydrated. The process seems to evolve with time under saturated conditions, in agreement with the postulated disaggregation of smectite tactoids and the relative increase of specific surface from partly hydrated to full saturated conditions. Unfortunately, under saline conditions, the increase of birefringece is not produced at a general scale.

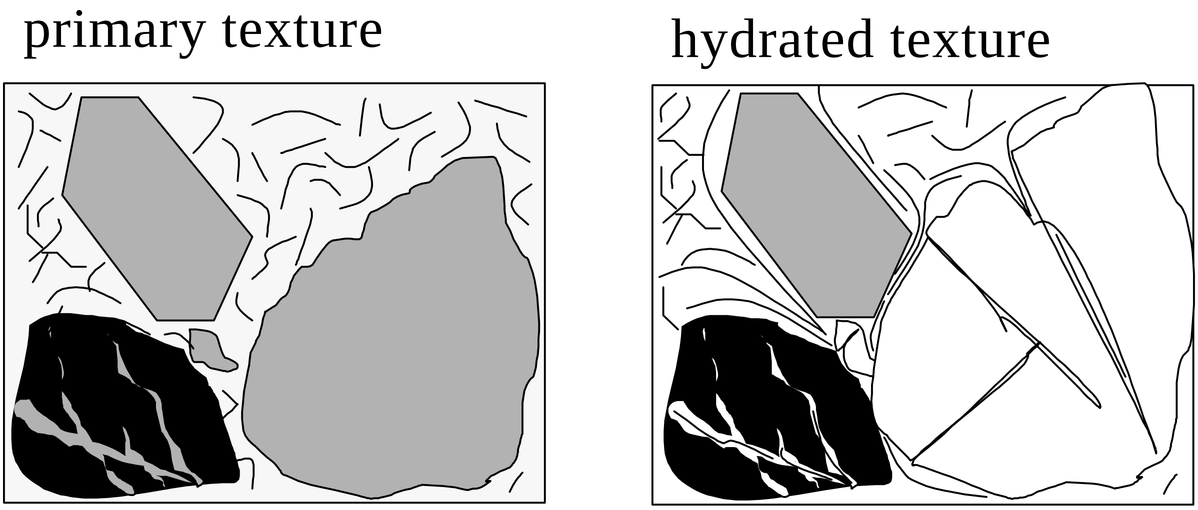

Figure 25. Idealised sketch of the hydration effects in the clay. Black fragment: vitreous volcanic rock; polygonal fragment: microcrystal; grey to white-grey fragment: smectite aggregate; lines and dots: oriented and random arrangements.

6.2.3. Quantification of calcite precipitates

The determination of the quantities of calcite precipitates has been done through more than 200 hundred fields of observation per F (fabric) test (40 fields per slice). Both sparitic cements on feldspars or micritic deposits have been quantified. Figure 26 shows the bulk quantities in each test without distinction between the types of precipitates. There was no systematic relationship to the position of the slice under low gradient conditions. At high temperature, greater amount of calcite have been observed near the heater, especially in the tests with granitic water.

All the measurements on F treated samples have calcite crystals with greater area than the original bentonite. The calcite may be redistributed by dissolution-precipitation. This does not necessarily mean that the bulk calcite content has increased, since calcite can “spread” along the sample. This “spreading” effect is possible by partial dissolution of sparitic crystals and subsequent precipitation at sites not far from the original position.

There were two disctinct behaviours depending on the kind of water used. Calcite seems to be leached with time in the more diluted granitic environment. Saline water produces the opposite effect. Calcite occupies more “area” as the time of the test is increased. The time is the key variable in this process instead of temperature.

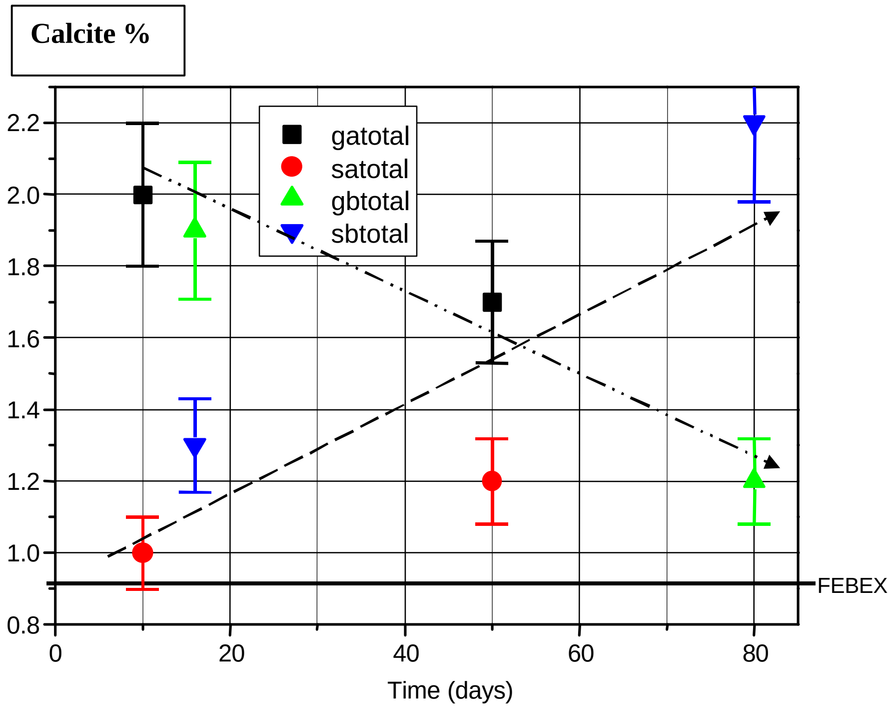

Figure 26: Total amount of calcite precipitates as determined by area measurement under a semiautomatic image analysis. Points are the average data from the 5 slices quantified in each F test (g: granitic, s: saline, a: high temperature, b: low temperature)

7. PERMEABILITY MEASUREMENTS

Once the thermo-hydraulic treatment is finished, the hydraulic conductivity of the sample is determined at laboratory temperature. The sample is extracted from the Teflon cell and trimmed to fit into the permeability cell, which is a stainless steel cylinder of inner diameter 5.0 cm and inner height 2.5 cm, in which the sample is confined on top and bottom by porous stones. The permeability measurements have been done only on samples treated during times longer than the saturation time, but, anyway, the saturation of the clay in the permeability cell is assured by injecting water at a pressure of 0.6 MPa by both ends during two days. Afterwards, the injection pressure at the bottom of the specimen is increased to 4.7 MPa, resulting in a hydraulic gradient of 16400. The water outflow is measured as a function of time and the hydraulic conductivity is calculated by applying Darcy's law. The determinations have been performed using as permeant the same kind of water used during the thermo-hydraulic treatment, granitic or saline. The general procedure followed is that described in Villar (1997).

The hydraulic conductivity values obtained (K, m/s) for samples previously subjected to thermo-hydraulic treatment are shown in Figure 27 as a function of their dry densities (ρ_d, g/cm^3). The variation of the dry density among different specimens is due to the trimming process, that induces also a density decrease with respect to that of the clay in the TH cell. The values obtained are also compared to those that would have been obtained for a non-treated sample of the same dry density, according to the relationship shown in the section "Hydromechanical properties". The percentage of deviation has been calculated as the difference between the actual and the theoretical value with respect to the theoretical value. Consequently, negative values of deviation indicate that the obtained value is lower than the theoretical one and vice versa. When comparing the obtained values to the theoretical ones, two facts must be taken into account:

- This relationship was obtained for tests with untreated samples in which distilled water was used as permeant. No differences were found between tests performed with distilled or granitic water. However, the permeability values obtained with saline water as permeant are a 71 % higher than those for distilled water.

- The fitting for untreated samples was obtained in specimens compacted inside the permeability cell, while the treated samples have been trimmed and subsequently introduced in the cell. When a trimmed sample is introduced in the permeability cell, the fitting between the specimen and the cell walls is not perfect at the beginning of the test, and the bentonite swells as it is resaturated, causing a density decrease which is very important just in the outer part of the specimen, although the whole of the sample keeps almost its initial dry density, which is the one that controls the flow of water as a function of time and consequently, the permeability measured. On the computation of the final dry density of a trimmed sample, an average density is obtained, supposing a homogeneous density, which is lower than the actual density of most of the sample (except for the borders). For this reason, the permeability values measured on trimmed samples are always lower than those expected for samples of the same homogeneous dry density compacted inside the permeability cell. Experiments performed with this bentonite have shown that the permeability values measured for trimmed samples may be in the order of 17% lower than those for compacted samples of the same dry density (Villar 1999c).

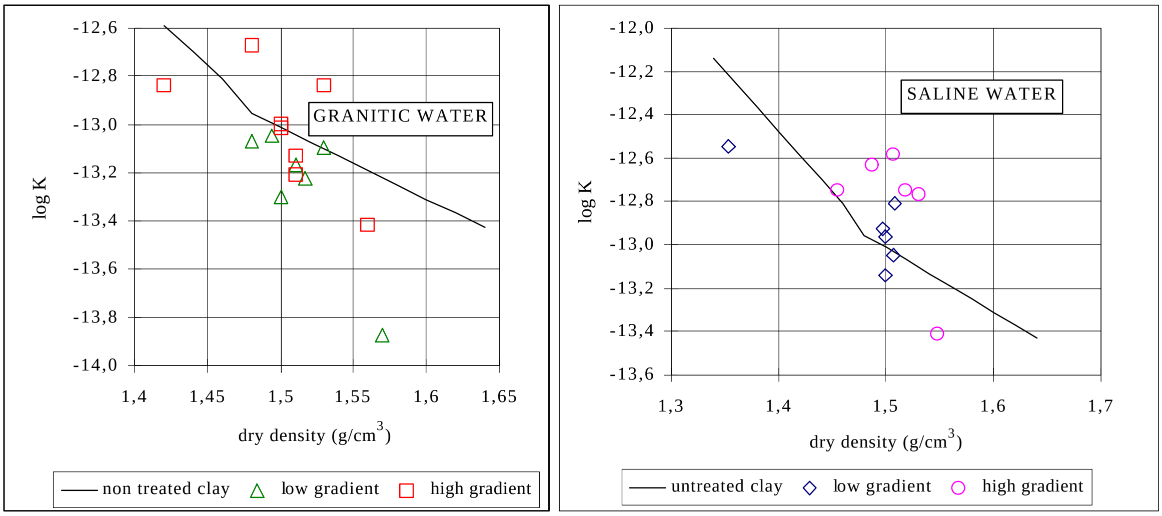

Figure 27. Hydraulic conductivity values (K in m/s) obtained for samples previously hydrated with granitic or saline water under different thermal gradients and comparison with the theoretical values for an untreated sample

Figure 28 shows the percentage of deviation of the measured permeability value with respect to the theoretical value for an untreated sample of the same dry density, expressed as a function of the duration of the thermo-hydraulic treatment and of the thermal gradient applied. The behaviour of the samples depends on the kind of saturation water.

The values obtained for samples treated under high thermal gradient with granitic water are an 11 % higher than the theoretical ones for non-treated samples saturated with distilled water and compacted inside the permeability cell. The samples treated with granitic water under low thermal gradient have permeabilities a 31 % lower than the theoretical ones for non-treated samples, i.e., only slightly lower than what could be expected on the basis of the differences on sample preparation (trimming or compaction inside the cell, respectively). No tendencies with respect to the duration of treatment can be observed.

For samples hydrated with saline water under a high thermal gradient, the hydraulic conductivities measured are an 85 % higher than the theoretical ones for samples of the same dry density compacted inside the permeability cell and saturated with distilled water. For the samples hydrated with saline water under a low thermal gradient the hydraulic conductivities measured are only a 13 % higher than the theoretical ones for distilled water, what in fact implies a reduction of hydraulic conductivity with respect to that of untreated samples tested with saline water as permeant. The influence of the duration of TH treatment on the modification of the hydraulic conductivity is not clear: for the tests performed with saline water at high gradient, there seems to be a reduction of permeability as a function of time, what would correlate with the results obtained for the specific surface, that increases with the duration of treatment.

Summarising: certain increase of the hydraulic conductivity has been observed after thermo-hydraulic treatment at high temperature for up to 80 days, either with granitic or saline water, this increase being more important when saline water is used, even for short periods of treatment. However, for the tests under low temperature, specially in the case of saline water, the permeability seems to slightly decrease after the TH treatment.

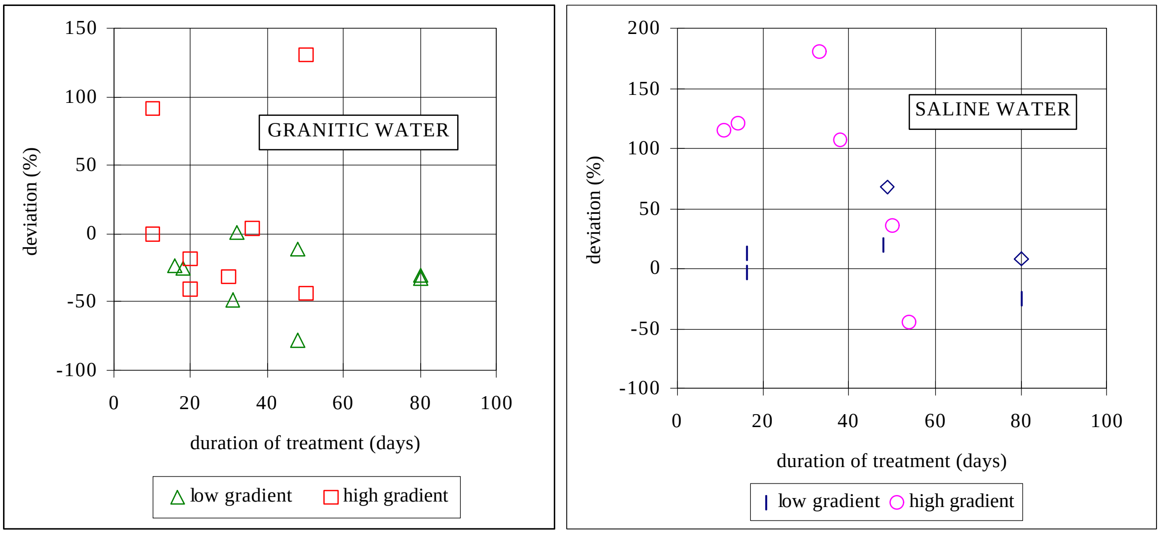

Figure 28. Deviation of the permeability values obtained for samples hydrated with granitic or saline water under different thermal gradients with respect to the theoretical values for untreated samples of the same dry density

8. SWELLING CAPACITY

In some of the tests longer than the saturation time, once the thermo-hydraulic treatment is finished, the clay is stabilised at laboratory conditions in order to attain an equilibrium water content, which lies between 14 and 16%. Afterwards, the clay is gently disaggregated. With this material, new specimens of dry density 1.60 g/cm^3 are prepared by uniaxial compaction in the oedometer ring. The aim of this preparation is to have analogous initial conditions in all the samples, what can not be reached when trimmed samples are used. A disadvantage of this method of preparation is that it does not allow checking the influence of possible weak cementations that would be broken during the remoulding (Oscarson et al. 1990).

For every kind of TH treatment, i.e., of a given duration, thermal gradient and kind of water, four tests of saturation under a constant vertical load are performed with the remoulded sample. The vertical loads applied are 0.1, 0.5, 1.0 and 3.0 MPa, and the samples are saturated with the same kind of water used during the TH treatment. The ring with the compacted sample inside is placed in the oedometer cell and the vertical load is applied. Water is poured into the cell just to cover the lower porous stone so that saturation take place from bottom to top, and the vertical deformation is registered as a function of time. The duration of the swelling tests ranges between 7 and 15 days, and they are conducted as detailed in Villar (2000).

The results obtained are shown in Figure 29, together with the fittings obtained for untreated samples compacted to dry density 1.60 g/cm^3 with the equilibrium water content at laboratory conditions and saturated either with granitic or saline water (see section “Hydromechanical properties”). The thermal gradient applied, high or low, during the TH treatment is indicated, but not the duration of the TH treatment, as no modification of the behaviour of the samples can be observed as a function of this parameter.

All the samples saturated with granitic water show a higher swelling capacity (higher strain upon saturation) after being subjected to TH treatment. The samples that had been saturated under a high thermal gradient show a 92% deviation with respect to the values expected for untreated samples, while the samples that had been saturated under a low thermal gradient show a 49% deviation with respect to the values expected for untreated samples.

On the contrary, no modification of the swelling capacity before and after the TH treatment has been observed for the samples saturated with saline water.

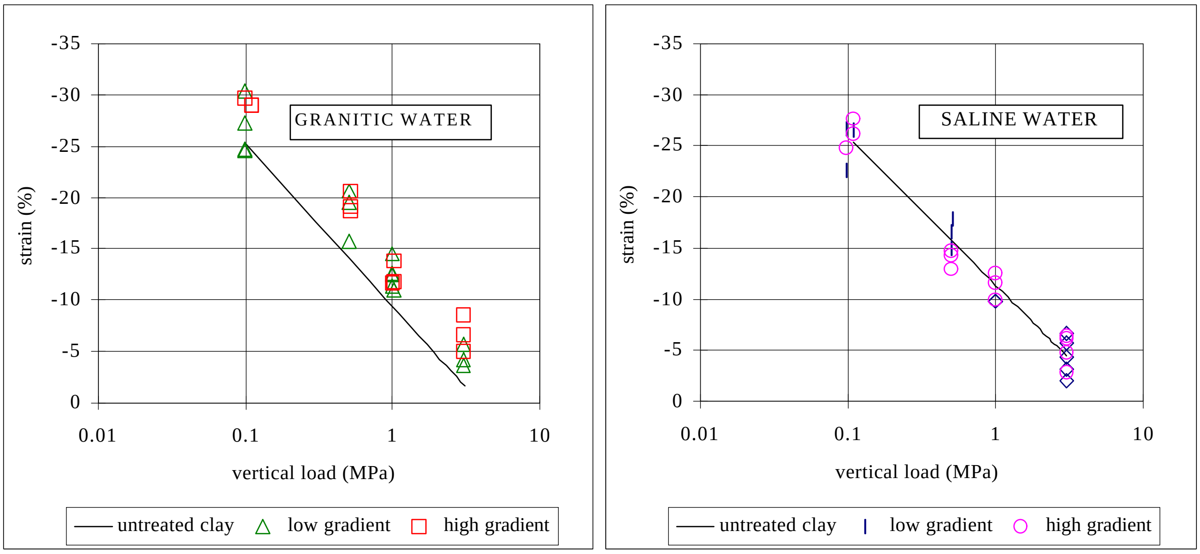

Figure 29. Strain upon saturation under constant vertical load for remoulded clay (initial ρ_d=1.60 g/cm^3 and w=14%) previously hydrated (granitic or saline water) under thermal gradient (low or high), and comparison with the values expected for an untreated sample of the same characteristics

This behaviour suggests that during the hydration with granitic water the cementing agents are dissolved, specially if temperature is high, allowing a higher swelling of the sample when it is put in contact with water again in the oedometer test. This is in agreement with the microstructural rearrangement inferred by means of optical observations. On the contrary, no modification of the swelling capacity is observed when hydration takes place with saline water, what implies a lower influence in the disruption of cemented aggregates.

9. CONCLUSIONS

The role of the geochemical environment and of the microstructure modifications during thermo-hydraulic treatment of the bentonite on its hydraulic and mechanical behaviour has been tested. A NaCl loaded water front is developed during the hydration stage, mainly due to the simultaneous advective transport and dissolution of salts inside the bentonite. This phenomenon is favoured by rising the average temperature and is not dependent on the salinity of the circulating water. The small impact of the salinity of water in this process is attributable to the inhibition of anion transport once the bentonite is saturated near the hydration source.

A net decrease of bulk salinity is detected from the beginning of hydration both in saline and granitic conditions, more significant at higher temperatures. The rapid lost of salts implies a very efficient anion transport outside the bentonite, that could be accelerated by the existence of preferential passages. The driving force for this transport out of the bentonite would be the increase of salt concentration on the mesopore “external” water with respect to the “surface influenced” (anion exclusion) micropore water. The preservation of primitive interfaces upon saturation in the bentonite has been observed by optical-polarising microscopy, what can be a proof of the maintenance of preferential pathways for salt migration. The only permanent concentration gradient that has been observed is that at the hydration interface in the experiments with saline water.

Consequently, the compacted bentonite has a limited capability to behave as a salt reservoir at saturation. For this reason, no or little impacts on hydraulic conductivity or swelling pressure should be expected when the bentonite is completely saturated, due to the low solute concentrations and the constancy in the distribution of exchangeable cations observed (although some replacement of Na by Ca in the exchange complex may exist).

In the short-term, the hydraulic conductivity of the clay increases slightly after TH treatment under high temperature with granitic and, especially, saline water. In the case of saline water, this increase becomes lower with the duration of treatment, what could be related to the general decrease of salinity with time. The swelling capacity of the remoulded clay increases after TH treatment with granitic water, and remains unchanged when saline water is used. This increase might be related to the dissolution of cementing agents by the granitic water, which would bring a disaggregation of bentonite flakes what seems to be confirmed by the microstructural observations. This is also consistent with the calcite leaching observed by optical microscopy.

The influence of the thermo-hydraulic treatment on the behaviour of the clay seems to be affected mainly by the kind of water used to saturate the sample and, to a lesser extent, by the temperature applied during saturation. For the periods of time studied (up to 80 days), no influence of the duration of the treatment on the subsequent physical behaviour of the clay has been detected, what may imply that the possible modifications occur at the very beginning or at longer times. None of the observed modifications will have a major repercussion on the performance of the clay barrier, as the properties remain in the required range for suitability of the material.

The effect of the spatial and time scale of these tests with respect to the actual scale of the clay barrier must be taken into account in the analysis of the results obtained; the major difference being that the clay saturates quickly in the TH cells while it will remain unsaturated for long periods of time in the repository. The short-distance/short-time scales of these experiments accelerate saturation and ion transport phenomena what may hide the long-term alteration produced during the high temperature/low water content transient period near the heater. This can prevent the development of precipitated calcite films at the water front or other negative surface effects on the smectites, as the loss of swelling capacity. This aspect will be envisaged in another set of TH tests.

10. ACKNOWLEDGEMENTS

This work has been supported by ENRESA and EC through contract FI4W-CT95-006. A. Pelayo, J. Aroz and R. Campos from CIEMAT performed part of the laboratory work. G. Rincón from UAM manufactured the thin sections.

11. REFERENCES

BARAHONA, E. (1974): Arcillas de ladrillería de la provincia de Granada. Evaluación de algunos ensayos de materias primas. *Tesis doctoral Universidad de Granada*. Secr. Public. no 49, 398 pp.

COBEÑA, J.C.; MARTÍN, M.; RAMÍREZ, S.; VIGIL DE LA VILLA, R.; CUEVAS, J. & LEGUEY, S.(1998): Estudio detallado de la mineralogía y microestructura de una bentonita sometida a procesos de calentamiento e hidratación. *XVIII Reunion de la Sociedad Española de Mineralogía*. Abstracts.

CUEVAS, J. & MARTÍN, M.(1998): Ensayos THG en celdas. Resultados de los ensayos en celdas pequeñas de transporte con agua granítica. CIEMAT/DIAE/54111/8/98. FEBEX report 70-IMA-L-0-54.

CUEVAS, J. & MARTÍN, M.(1999): Ensayos THG en celdas. Resultados de los ensayos de transporte con agua salina. CIEMAT/DIAE/54111/6/99. FEBEX report 70-IMA-L-0-63.

CUEVAS, J & VILLAR, M.V.(1997): Diseño y fabricación del equipo experimental para ensayos termo-hidro-geoquímicos en celdas pequeñas. *Informe Técnico CIEMAT-IMA 54A15/5/97*. 70-IMA-L-0-38. 10 pp.

CUEVAS, J.; COBEÑA, J.C. & MARTÍN, M.(1999): Ensayos THG en celdas. Resultados de los ensayos de fábrica con agua granítica y salina. CIEMAT/DIAE/54111/7/99. FEBEX report 70-IMA-L-0-64.

CUEVAS, J.; VILLAR, M.V. & HIDALGO, D.(1997): Metodología de los ensayos termo-hidro-geoquímicos en celdas pequeñas. *Informe Técnico CIEMAT-DIAE* 54A10/4/97. 70-IMA-L-0-47.

CUEVAS, J.; VILLAR, M.V.; FERNÁNDEZ, A.M.; GÓMEZ, P. & MARTÍN, P.L.(1997): Pore waters extracted from compacted bentonite subjected to simultaneous heating and hydration. *Applied Geochemistry* 12: 473-481.

DREES, L.R. & RANSOM, M.D. (1994): Light microscopic techniques in quantitative soil mineralogy. En: J.E. Amonette and L.W. Zelany (editores) “Quantitative Methods in Soil Mineralogy”. *SSSA Miscellaneous Publication*. SSSA.Madison, Wisconsin, USA. 137-171.

DUDOIGNON, P., PANTET, A. (1998): Measurement and cartography of clay matrix orientations by image analysis and grey level diagrm descomposition. *Clay Minerals*. Vol. 33, 629-642.

ENRESA (1997): FEBEX. Etapa preoperacional. Informe de síntesis. *Publicación Técnica* 9/97. 189 pp. Madrid.

ENRESA (1998): FEBEX. Bentonite: origin, properties and fabrication of blocks. *Publicación Técnica* 4/98. Madrid.

FERNÁNDEZ, A.M. & CUEVAS, J.(1998): Estudios del agua intersticial de la arcilla FEBEX. *Internal report CIEMAT*. 70-IMA-L-9-44.

IDEMITSU, K.; TACHI, Y.; FURUYA, H.; INAGAKI, Y.; ARIMA, T. (1998): Diffusion of Cs and Sr in compacted bentonite under reducing conditions and in the presence of corrosion products of iron. MRS Symposium Proceedings Scientific Basis for Nuclear Waste Management XXI (506): 351-358.

KHARAKA, Y.K. & BERRY, F.A.(1973): Simultaneous flow of water and solutes through geological membranes-I. Experimental investigation. *Geochimica et Cosmochimica Acta* 37: 2577-2603.

KIM, J.; PEACOR, D.R.; TESSIER, D. & ELSASS, F.(1995): A technique for mantaining texture and permanent expansion of smectite interlayer for TEM observations. *Clays and Clay Minerals* 43: 51-57.

MADSEN, F.T. (1998): Clay mineralogical investigations related to nuclear waste disposal. *Clay Miner*. Vol. 33(1): 109-129.

MADSEN, F.T. AND KAHR, G. (1993): Diffusion of ions in compacted bentonite. *Proc. Intl. Conf. Nuclear Waste Management and Environmental.*

ROBINSON, R.A.& STOKES,R.H. (1959). Electrolitic solutions. *Butterwoths*. London.

MELAMED, A.; PITKÄNEN, P.; OLIN, M.; MUURINEN, A. & SNELLMAN, M.(1992): Interaction of water and compacted sodium-bentonite in simulated nuclear waste disposal conditions. *Mat. Res. Soc. Symp. Proc.* 257: 557-566.

MUURINEN, A. & LEHIKOINEN, J.(1997): Evolution of the porewater chemistry in compacted bentonite. *MRS Symposium Proceedings Scientific Basis for Nuclear Waste Management XXI* (506): 415-422.

OSCARSON, D.W.; DIXON, D.A. & GRAY, M.N.(1990): Swelling capacity and permeability of an unprocessed and a processed bentonitic clay. *Engineering Geology* 28: 281-289.

PUSCH, R.(1985): Final Report of the Buffer Mass Test- Volume III: Chemical and physical stability of the buffer materials. *Stripa Project Technical Report* 85-14. SKB. 65 pp.

SCHULTZ, L.G. (1964): Quantitative interpretation of the mineralogical composition from x-ray and chemical data for the Pierre Shale. *U. S. Geol. Surv. Prof. Pap.* 391C.

SPOSITO, G.(1992): The diffuse ion swarm near smectite particles. In: Clay–water interface and its rheological implications. *CMS Workshop Lecture Series* 4: 127-156. CMS. Colorado. USA.

THOMAS, W.G.(1982): Exchangeable cations. In: Methods of soil analysis, Part 2, Chemical and Microbiological properties. *ASA-SSSA*. Madison Wisconsin, USA.

VILLAR, M.V.(1997): Permeabilidad de materiales expansivos. *Procedimiento específico CIEMAT* IMA/X8/BI-F14. (70-IMA-G-0-14).

VILLAR, M.V.(1999a): Ensayos THG en celdas. Resultados de los ensayos de permeabilidad e hinchamiento con agua salina. CIEMAT/DIAE/54111/5/99. FEBEX report 70-IMA-L-0-65.

VILLAR, M.V.(1999b): Ensayos THG en celdas. Resultados de los ensayos de permeabilidad e hinchamiento con agua granítica. CIEMAT/DIAE/54111/8/99. FEBEX report 70-IMA-L-0-55.

VILLAR, M.V.(1999c): Ensayos THM para el proyecto FEBEX. Versión 0. CIEMAT/DIAE/54111/9/99. FEBEX REPORT 70-IMA-L-0-66.

VILLAR, M.V. (2000): Hinchamiento bajo carga. *Procedimiento específico CIEMAT* PE-IA-CH-03. (70-IMA-G-0-20).

VILLAR, M.V., CUEVAS, J. & MARTÍN, P.L.(1996): Effects of heat/water flow interaction on compacted bentonite: Preliminary results. *Engineering Geology* 41: 257-267.